Contents lists available at ScienceDirect

International Journal of Solids and Structures

journal homepage: www.elsevier.com/locate/ijsolstr

The minimal error method for the Cauchy problem in linear elasticity. Numerical implementation for two-dimensional homogeneous isotropic linear elasticity

Liviu Marin *

Institute of Solid Mechanics, Romanian Academy, 15 Constantin Mille, Sector 1, P.O. Box 1-863, RO-010141 Bucharest, Romania

A R T I C L E   I N F O

A B S T R A C T

In this paper, yet another iterative procedure, namely the minimal error method (MEM), for solving stably the Cauchy problem in linear elasticity is introduced and investigated. Furthermore, this method is compared with another two iterative algorithms, i.e. the conjugate gradient (CGM) and Landweber–Fridman methods (LFM), previously proposed by Marin et al. [Marin, L., Háo, D.N., Lesnic, D., 2002b. Conjugate gradient-boundary element method for the Cauchy problem in elasticity. Quarterly Journal of Mechanics and Applied Mathematics 55, 227–247] and Marin and Lesnic [Marin, L., Lesnic, D., 2005. Boundary element-Landweber method for the Cauchy problem in linear elasticity. IMA Journal of Applied Mathematics 18, 817–825], respectively, in the case of two-dimensional homogeneous isotropic linear elasticity. The inverse problem analysed in this paper is regularized by providing an efficient stopping criterion that ceases the iterative process in order to retrieve stable numerical solutions. The numerical implementation of the aforementioned iterative algorithms is realized by employing the boundary element method (BEM) for two-dimensional homogeneous isotropic linear elastic materials.

1. Introduction

Over the last decades, special attention has been given to *inverse problems* related to the mechanics and fracture of solids and structures, see e.g. Kubo (1988) and Yakhno (1990). Compared to *direct problems* in solid mechanics, for which the governing system of partial differential equations (equilibrium equations), the constitutive and kinematics equations, the initial and boundary conditions for the displacement and/or traction vectors and the geometry of the domain occupied by the solid are all known, inverse problems may be characterized by the lack of at least one of the conditions enumerated above. Another major difference for these two classes of problems is represented by the fact that while for direct problems the existence and uniqueness of their solutions have been well established, see for example Knops and Payne (1986), inverse problems are in general ill-posed, i.e. the existence, uniqueness and stability of their solutions are not always guaranteed, see e.g. Hadamard (1923).

A classical example of an inverse boundary value problem in solid mechanics is represented by the Cauchy problem. In this case, boundary conditions are incomplete, in the sense that a part of the boundary of the domain occupied by the solid is over-specified by prescribing on it both the displacement and traction vectors, whilst the remaining boundary is under-specified and boundary conditions on the latter boundary have to be determined. Maniatty et al. (1989) have used simple diagonal regularization, in conjunction with the finite element method (FEM), to determine the traction boundary

---

* Tel.: +40 745 461023.
  E-mail address: marin.liviu@gmail.com

condition. Spatial regularization has been introduced in conjunction with the boundary element method (BEM) by Zabaras et al. (1989) and with the FEM by Schnur and Zabaras (1990). The Cauchy problem in elasticity has also been studied theoretically by Yeih et al. (1993), who have analysed its existence, uniqueness and continuous dependence on the data and have proposed an alternative regularization procedure, namely the fictitious boundary indirect method, based on the simple or double layer potential theory. The numerical implementation of the aforementioned method has been undertaken by Koya et al. (1993), who have used the BEM and the Nyström method for discretising the integrals. However, this formulation has not yet removed the problem of multiple integrations. Marin et al. (2001) have determined the approximate solutions to the Cauchy problem in isotropic linear elasticity using an alternating iterative BEM which reduced the problem to solving a sequence of well-posed boundary value problems. Latter, this method has been implemented for anisotropic linear elastic materials by Comino et al. (2007). Huang and Shih (1997), Marin et al. (2002b), and Marin and Lesnic (2002a) have used both the conjugate gradient method (CGM) and the Tikhonov regularization method combined with the BEM, in order to solve the same problem. The singular value decomposition (SVD), in conjunction with the BEM, has been employed by Marin and Lesnic (2002b) to determine the numerical solutions to Cauchy problems in linear elasticity. Four regularization methods for solving stably the Cauchy problem in linear elasticity, namely the Tikhonov regularization, the SVD, the CGM and an alternating iterative algorithm implemented by Marin et al. (2001), have been compared in Marin et al. (2002a). It was found in (Marin et al., 2002a) that the truncated SVD outperforms the Tikhonov regularization method, whilst the later outperforms the CGM. Marin and Lesnic (2004) and Marin (2005) have proposed a meshless method, namely the method of fundamental solutions, in conjunction with the Tikhonov regularization method, for solving the Cauchy problem in two- and three-dimensional isotropic linear elasticity, respectively. The Cauchy problem in elasticity with L^2-boundary data has been approached by Marin and Lesnic (2005) by combining the Landweber–Fridman method (LFM), see Landweber (1951), with the BEM.

It is important to mention that the non-iterative Tikhonov regularization and truncated SVD methods may produce numerical solutions even when the original Cauchy problem does not have a classical solution, whilst the alternating iterative algorithm described and implemented in Marin et al. (2001) is convergent only if the differential operator associated with the governing equation is positive (or negative) definite and self-adjoint. Therefore, for Cauchy problems with disjoint under- and over-specified boundaries the most common methods would be the CGM, LFM and the minimal error method (MEM), see e.g. King (1989). The main advantage of these methods is that they can be reformulated for L^2-boundary data, a very desirable feature from the computational point of view. Furthermore, these three algorithms being iterative methods, it is expected that for exact data they are convergent if and only if the solution of the original Cauchy problem exists. One possible disadvantage of the LFM over the CGM and MEM is represented by the fact that the former is a parameter-dependent method. Consequently, special care should be taken when choosing the parameter associated with the LFM, so that the convergence of this iterative method would be ensured, and this may result in a very large number of iterations performed and hence large computational time.

Motivated by these facts and encouraged by the recent results of Johansson and Lesnic (2006b) obtained for the MEM applied to the Cauchy problem associated with the Stokes system in hydrostatics, we decided present and analyse in this paper yet another iterative method for solving the Cauchy problem in linear elasticity, namely the MEM. This iterative method reduces the original Cauchy problem to solving a sequence of two well-posed mixed boundary value problems. It is also proven in this study that, accompanied by a suitable stopping criterion, the MEM has a regularizing/stabilising character. Furthermore, it is shown that this method is very suitable for solving the Cauchy problem in linear elasticity since only a few iterations are required to obtain a stable and accurate numerical solution.

The paper is organised as follows: Section 2 is devoted to the mathematical formulation of the inverse problem investigated in the general linear elasticity framework. The LFM applied to solving the Cauchy problem in linear elasticity, as well as the associated operators, direct and adjoint problems, and convergence theorem, are briefly presented in Section 3. Next section, describes the alternatives to the parameter-dependent method described previously, namely the CGM and MEM that are presented in Sections 4.1 and 4.2, respectively. In Section 5, the MEM is applied to solving three Cauchy problems with and without noisy Cauchy data, for an isotropic linear elastic material occupying a two-dimensional doubly connected domain, as described in Section 5.1. The MEM is implemented using the BEM, as presented in Section 5.2, while at the same time the convergence, stopping regularizing criterion and stability of the method are numerically investigated in Sections 5.3–5.5, respectively. A comparison of the proposed iterative method with the CGM and LFM, previously analysed by Marin et al. (2002b) and Marin and Lesnic (2005), respectively, is made in Section 5.6. Finally, concluding remarks are provided in Section 6.

2. Mathematical formulation

Consider a homogeneous linear elastic material which occupies a bounded domain $\Omega \subset \mathbb{R}^d$, where usually $d \in \{1, 2, 3\}$, with the boundary $\Gamma = \partial\Omega$ of class $\mathscr{C}^2$. We also assume that the boundary consists of two parts, $\Gamma = \overline{\Gamma}_1 \cup \overline{\Gamma}_2$, where $\Gamma_1, \Gamma_2 \neq \emptyset$, and $\overline{\Gamma}_1 \cap \overline{\Gamma}_2 = \emptyset$. In the absence of body forces, the equilibrium equations are given by, see e.g. Landau and Lifshits (1986),

$$\mathscr{L}\mathbf{u}(\mathbf{x}) \equiv -\nabla \cdot \boldsymbol{\sigma}(\mathbf{u}(\mathbf{x})) = \mathbf{0}, \qquad \mathbf{x} \in \Omega. \tag{1}$$

Here, $\mathscr{L}$ is the Lamé (Navier) differential operator, $\boldsymbol{\sigma}(\mathbf{u}(\mathbf{x})) = [\sigma_{ij}(\mathbf{u}(\mathbf{x}))]_{1 \leqslant i,j, \leqslant d}$ is the stress tensor associated with the displacement vector $\mathbf{u}(\mathbf{x}) = (u_1(\mathbf{x}), \ldots, u_d(\mathbf{x}))^{\mathrm{T}}$, whilst on assuming small deformations, the corresponding strain tensor $\boldsymbol{\varepsilon}(\mathbf{u}(\mathbf{x})) = [\varepsilon_{ij}(\mathbf{u}(\mathbf{x}))]_{1 \leqslant i,j, \leqslant d}$ is given by the kinematic relations

$$\boldsymbol{\varepsilon}(\mathbf{u}(\mathbf{x})) = \frac{1}{2}(\nabla \mathbf{u}(\mathbf{x}) + \nabla \mathbf{u}(\mathbf{x})^{\mathrm{T}}), \qquad \mathbf{x} \in \overline{\Omega} = \Omega \cup \Gamma. \tag{2}$$

These tensors are related by the constitutive law, namely

$$\boldsymbol{\sigma}(\mathbf{u}(\mathbf{x})) = \mathbf{C}\boldsymbol{\varepsilon}(\mathbf{u}(\mathbf{x})), \qquad \mathbf{x} \in \overline{\Omega}, \tag{3}$$

where $\mathbf{C} = [C_{ijkl}]_{1 \leqslant i,j,k,l \leqslant d}$ is the fourth-order elasticity tensor which is symmetric and positive definite.

We now let $\mathbf{n}(\mathbf{x}) = (n_1(\mathbf{x}), \ldots, n_d(\mathbf{x}))^{\mathrm{T}}$ be the outward normal vector at $\mathbf{x} \in \Gamma$ and $\mathscr{N}\mathbf{u}(\mathbf{x}) \equiv \mathbf{t}(\mathbf{x}) = (t_1(\mathbf{x}), \ldots, t_d(\mathbf{x}))^{\mathrm{T}}$ be the traction vector at a point $\mathbf{x} \in \Gamma$ defined by

$$\mathscr{N}\mathbf{u}(\mathbf{x}) \equiv \mathbf{t}(\mathbf{x}) = \boldsymbol{\sigma}(\mathbf{u}(\mathbf{x})) \cdot \mathbf{n}(\mathbf{x}), \qquad \mathbf{x} \in \Gamma, \tag{4}$$

where $\mathscr{N}$ is the boundary-differential operator associated with the Lamé (Navier) differential operator, $\mathscr{L}$, and Neumann boundary conditions on Γ. In the direct problem formulation, the knowledge of the displacement and/or traction vectors on the whole boundary Γ gives the corresponding Dirichlet, Neumann, or mixed boundary conditions which enable us to determine the displacement vector in the domain Ω. Then, the strain tensor, $\boldsymbol{\varepsilon}$, can be calculated from Eq. (2) and the stress tensor, $\boldsymbol{\sigma}$, is determined using the constitutive law (3).

If it is possible to measure both the displacement and traction vectors on a part of the boundary Γ, say Γ_0, then this leads to the mathematical formulation of the Cauchy problem consisting of the partial differential equation (1) and the boundary conditions

$$\mathbf{u}(\mathbf{x}) = \boldsymbol{\varphi}(\mathbf{x}), \quad \mathscr{N}\mathbf{u}(\mathbf{x}) \equiv \mathbf{t}(\mathbf{x}) = \boldsymbol{\psi}(\mathbf{x}), \qquad \mathbf{x} \in \Gamma_0, \tag{5}$$

where $\boldsymbol{\varphi} \in L^2(\Gamma_0)^d$ and $\boldsymbol{\psi} \in L^2(\Gamma_0)^d$ are prescribed vector valued functions. In the above formulation of the boundary conditions (5), it can be seen that the boundary Γ_0 is over-specified by prescribing both the displacement $\mathbf{u}|_{\Gamma_0} = \boldsymbol{\varphi}$ and the traction $\mathbf{t}|_{\Gamma_0} = \boldsymbol{\psi}$ vectors, whilst the boundary Γ_1 is under-specified since both the displacement $\mathbf{u}|_{\Gamma_1}$ and the traction $\mathbf{t}|_{\Gamma_1}$ vectors are unknown and have to be determined. Hence on using relations (1)–(5), the Cauchy problem under investigation may be recast as

$$\begin{cases} \mathscr{L}\mathbf{u}(\mathbf{x}) = \mathbf{0}, & \mathbf{x} \in \Omega, \\ \mathbf{u}(\mathbf{x}) = \boldsymbol{\varphi}(\mathbf{x}), & \mathbf{x} \in \Gamma_0, \\ \mathscr{N}\mathbf{u}(\mathbf{x}) = \boldsymbol{\psi}(\mathbf{x}), & \mathbf{x} \in \Gamma_0. \end{cases} \tag{6}$$

It should be mentioned that in the case of a homogeneous isotropic linear elastic material, the components of the fourth-order elasticity tensor, $\mathbf{C}$, are given by

$$C_{ijkl} = G\left(\frac{2v}{1-v}\delta_{ij}\delta_{kl} + \delta_{ik}\delta_{jl} + \delta_{il}\delta_{jk}\right), \tag{7}$$

where G is the shear modulus, v is Poisson's ratio and δ_{ij} is the Kronecker delta tensor. Consequently, the constitutive law for homogeneous isotropic linear elastic materials can be expressed as

$$\boldsymbol{\sigma}(\mathbf{u}(\mathbf{x})) = G\left(\nabla \mathbf{u}(\mathbf{x}) + \nabla \mathbf{u}(\mathbf{x})^{\mathrm{T}}\right) + \frac{2vG}{1-v}(\nabla \cdot \mathbf{u}(\mathbf{x}))\mathbf{I}, \qquad \mathbf{x} \in \overline{\Omega}, \tag{8}$$

whilst the Lamé (Navier) differential operator, $\mathscr{L}$, and its corresponding boundary-differential operator associated with Neumann conditions, $\mathscr{N}$, given by relations (1) and (4), respectively, may be recast as

$$\mathscr{L}\mathbf{u}(\mathbf{x}) = -\nabla \cdot (G(\nabla \mathbf{u}(\mathbf{x}) + \nabla \mathbf{u}(\mathbf{x})^{\mathrm{T}})) + \nabla\left(\frac{2vG}{1-v}\nabla \cdot \mathbf{u}(\mathbf{x})\right), \qquad \mathbf{x} \in \Omega, \tag{9}$$

and

$$\mathscr{N}\mathbf{u}(\mathbf{x}) = \left[G(\nabla \mathbf{u}(\mathbf{x}) + \nabla \mathbf{u}(\mathbf{x})^{\mathrm{T}}) + \frac{2vG}{1-v}(\nabla \cdot \mathbf{u}(\mathbf{x}))\mathbf{I}\right] \cdot \mathbf{n}(\mathbf{x}), \qquad \mathbf{x} \in \Gamma, \tag{10}$$

respectively.

3. The Landweber–Fridman method

In this section, the operators, direct and adjoint problems, convergence theorem and numerical algorithm corresponding to the LFM applied to solving the Cauchy problem in linear elasticity are briefly presented. For more details, we refer the reader to Marin and Lesnic (2005).

3.1. Two direct problems and their associated linear operators

Consider the well-posed, mixed, direct problem for the Lamé (Navier) differential operator, $\mathscr{L}$, with zero Neumann boundary conditions on Γ_0 and non-zero L^2-Dirichlet boundary conditions on Γ_1, namely

$$\begin{cases} \mathscr{L}\mathbf{u}(\mathbf{x}) = \mathbf{0}, & \mathbf{x} \in \Omega, \\ \mathscr{N}\mathbf{u}(\mathbf{x}) = \mathbf{0}, & \mathbf{x} \in \Gamma_0, \\ \mathbf{u}(\mathbf{x}) = \boldsymbol{\eta}(\mathbf{x}), & \mathbf{x} \in \Gamma_1, \end{cases} \tag{11}$$

and the operator associated with this problem (11)

$$\mathscr{K} : L^2(\Gamma_1)^d \to L^2(\Gamma_0)^d, \qquad \boldsymbol{\eta} \in L^2(\Gamma_1)^d \to \mathscr{K}\boldsymbol{\eta} = \mathbf{u}|_{\Gamma_0} \in L^2(\Gamma_0)^d. \tag{12}$$

In a similar manner, consider the well-posed, mixed, direct problem for the Lamé (Navier) differential operator, $\mathscr{L}$, with non-zero L^2-Neumann boundary conditions on Γ_0 and zero Dirichlet boundary conditions on Γ_1, i.e.

$$\begin{cases} \mathscr{L}\mathbf{v}(\mathbf{x}) = \mathbf{0}, & \mathbf{x} \in \Omega, \\ \mathscr{N}\mathbf{v}(\mathbf{x}) = \boldsymbol{\psi}(\mathbf{x}), & \mathbf{x} \in \Gamma_0, \\ \mathbf{v}(\mathbf{x}) = \mathbf{0}, & \mathbf{x} \in \Gamma_1, \end{cases} \tag{13}$$

and its associated operator, namley

$$\mathscr{K}_1 : L^2(\Gamma_0)^d \to L^2(\Gamma_0)^d, \qquad \boldsymbol{\psi} \in L^2(\Gamma_0)^d \to \mathscr{K}_1\boldsymbol{\psi} = \mathbf{v}|_{\Gamma_0} \in L^2(\Gamma_0)^d. \tag{14}$$

It has been shown that the operators $\mathscr{K}$ and $\mathscr{K}_1$ defined by Eqs. (12) and (14), respectively, are well-defined, linear and bounded and, moreover, the operator $\mathscr{K}$ is also injective and compact, see Johansson (2000) and Marin and Lesnic (2005). At this stage, the following remarks should be made:

1. Finding a solution $\boldsymbol{\eta} \in L^2(\Gamma_1)^d$ to the Cauchy problem (6) is equivalent to finding a solution $\boldsymbol{\eta} \in L^2(\Gamma_1)^d$ to the following operator equation:

$$\mathscr{K}\boldsymbol{\eta} = \boldsymbol{\varphi} - \mathscr{K}_1\boldsymbol{\psi}. \tag{15}$$

2. If such a solution $\boldsymbol{\eta} \in L^2(\Gamma_1)^d$ to the Cauchy problem (6) exists then from the definitions (12) and (14) of the operators $\mathscr{K}$ and $\mathscr{K}_1$, respectively, it follows that

$$\mathbf{u}|_{\Gamma_0} = \boldsymbol{\varphi} - \mathbf{v}|_{\Gamma_0}, \tag{16}$$

where $\mathbf{u}$ is the solution to the direct problem (11), whilst $\mathbf{v}$ solves the direct problem (13).

3. Since $\mathscr{K}$ is a compact operator, it follows that its inverse $\mathscr{K}^{-1}$ is unbounded. Therefore, the operator equation (15) is ill-posed and needs to be regularized.

3.2. Adjoint operator

The Cauchy problem in linear elasticity is regularized by introducing the adjoint operator, $\mathscr{K}^*$, to the operator $\mathscr{K}$ and the corresponding adjoint problem and the relation between these two entities is specified in the following:

Lemma 1 (Marin and Lesnic, 2005 and Johansson, 2000). *Let $\boldsymbol{\xi} \in L^2(\Gamma_0)^d$. The adjoint operator, $\mathscr{K}^*$, to the operator $\mathscr{K}$ defined by Eq. (12) is given by*

$$\mathscr{K}^* : L^2(\Gamma_0)^d \to L^2(\Gamma_1)^d, \qquad \boldsymbol{\xi} \in L^2(\Gamma_0)^d \to \mathscr{K}^*\boldsymbol{\xi} = -\mathscr{N}^*\mathbf{v}|_{\Gamma_1} \in L^2(\Gamma_1)^d, \tag{17}$$

where $\mathbf{v} \in L^2(\Omega)^d$ is a solution to the adjoint problem

$$\begin{cases} \mathscr{L}^*\mathbf{v}(\mathbf{x}) = \mathbf{0}, & \mathbf{x} \in \Omega, \\ \mathscr{N}^*\mathbf{v}(\mathbf{x}) = \boldsymbol{\xi}(\mathbf{x}), & \mathbf{x} \in \Gamma_0, \\ \mathbf{v}(\mathbf{x}) = \mathbf{0}, & \mathbf{x} \in \Gamma_1. \end{cases} \tag{18}$$

It is very important to mention that $\mathscr{L}^* = \mathscr{L}$ and $\mathscr{N}^* = \mathscr{N}$ in the case of linear elasticity.

3.3. The Lanweber–Fridman method. Convergence theorem

The following iterative procedure for solving the Cauchy problem in linear elasticity has been proposed, analysed and implemented for two-dimensional isotropic linear elastic materials by Marin and Lesnic (2005):

Step 1. Set $k = 1$ and choose an arbitrary function $\boldsymbol{\eta}^{(k)} \in L^2(\Gamma_1)^d$.

Step 2. Solve the direct problem

$$\begin{cases} \mathscr{L}\mathbf{u}^{(k)}(\mathbf{x}) = \mathbf{0}, & \mathbf{x} \in \Omega, \\ \mathscr{N}\mathbf{u}^{(k)}(\mathbf{x}) \equiv \boldsymbol{\sigma}(\mathbf{u}^{(k)}(\mathbf{x})) \cdot \mathbf{n}(\mathbf{x}) = \boldsymbol{\psi}(\mathbf{x}), & \mathbf{x} \in \Gamma_0, \\ \mathbf{u}^{(k)}(\mathbf{x}) = \boldsymbol{\eta}^{(k)}(\mathbf{x}), & \mathbf{x} \in \Gamma_1, \end{cases} \tag{19}$$

to determine $\mathbf{u}^{(k)}(\mathbf{x})$, $\mathbf{x} \in \Omega$, and $\mathscr{N}\mathbf{u}^{(k)}(\mathbf{x}) \equiv \mathbf{t}^{(k)}(\mathbf{x})$, $\mathbf{x} \in \Gamma_1$. Set

$$\boldsymbol{\xi}^{(k)}(\mathbf{x}) = \boldsymbol{\varphi}(\mathbf{x}) - \mathbf{u}^{(k)}(\mathbf{x}), \qquad \mathbf{x} \in \Gamma_0. \tag{20}$$

Step 3. Solve the adjoint problem

$$\begin{cases} \mathscr{L}^*\mathbf{v}^{(k)}(\mathbf{x}) = \mathbf{0}, & \mathbf{x} \in \Omega, \\ \mathscr{N}^*\mathbf{v}^{(k)}(\mathbf{x}) \equiv \boldsymbol{\sigma}(\mathbf{v}^{(k)}(\mathbf{x})) \cdot \mathbf{n}(\mathbf{x}) = \boldsymbol{\xi}^{(k)}(\mathbf{x}), & \mathbf{x} \in \Gamma_0, \\ \mathbf{v}^{(k)}(\mathbf{x}) = \mathbf{0}, & \mathbf{x} \in \Gamma_1, \end{cases} \tag{21}$$

to update the unknown Dirichlet data on Γ_1 as

$$\boldsymbol{\eta}^{(k+1)}(\mathbf{x}) = \boldsymbol{\eta}^{(k)}(\mathbf{x}) - \gamma \mathscr{N}^*\mathbf{v}^{(k)}(\mathbf{x}), \qquad \mathbf{x} \in \Gamma_1, \tag{22}$$

where $0 < \gamma < |\mathscr{K}|^{-2}$.

Step 4. Set $k = k + 1$ and repeat Steps 2 and 3 until a prescribed stopping criterion is satisfied.

Finally, we mention the theorem claiming the convergence of the aforementioned iterative algorithm:

Theorem 1 (Marin and Lesnic, 2005). *Let* φ *and* ψ *be given in* $L^2(\Gamma_0)^d$. *Assume that the solution* $\mathbf{u} \in L^2(\Omega)^d$ *to the Cauchy problem (6) exists and choose* γ *such that* $0 < \gamma < |\mathscr{K}|^{-2}$. *Let* $\mathbf{u}^{(k)}$ *be the kth approximate solution to the algorithm described above. Then*

$$lim_{k\to\infty} \|\mathbf{u}^{(k)} - \mathbf{u}\|_{L^2(\Omega)^d} = 0, \tag{23}$$

for any initial data $\boldsymbol{\eta}^{(0)} \in L^2(\Gamma_1)^d$.

It follows from Engl et al. (1996) that the procedure presented above is the LFM, see also Landweber (1951), is a regularization method and therefore it works with approximate/noisy data. The LFM has been numerically implemented by Marin et al. (2004) for two-dimensional Helmholtz-type equations, Marin and Lesnic (2005) in the case of two-dimensional isotropic linear elastic materials, and Johansson and Lesnic (2007) for the Stokes system in hydrostatics.

4. Parameter-free methods

From a numerical point of view, it might be difficult to choose an appropriate value for the parameter γ in the right interval $(0, |\mathscr{K}|^{-2})$, so that the convergence of the LFM is ensured, see e.g. Theorem 1. In practice, this is achieved by choosing a very small value for the parameter $\gamma > 0$ (usually $\gamma \approx 0.1$) since the norm of the operator $\mathscr{K}$ is very difficult to be estimated. Consequently, as shown in Marin et al. (2004), Marin and Lesnic (2005), and Johansson and Lesnic (2007), in such cases the LFM becomes computationally very slow and in order to overcome this disadvantage, two parameter-free methods are proposed and described in the following.

Consider the operators $\mathscr{K}$ and $\mathscr{K}_1$ defined by Eqs. (12) and (14), respectively, and denote

$$\mathbf{y} \equiv \boldsymbol{\varphi} - \mathscr{K}_1 \boldsymbol{\psi}. \tag{24}$$

Then Eq. (15) becomes

$$\mathscr{K}\boldsymbol{\eta} = \mathbf{y}, \tag{25}$$

and the aim is to recover $\boldsymbol{\eta}$ for a given $\mathbf{y}$.

4.1. The conjugate gradient method

The CGM applied to solving the Cauchy problem in linear elasticity (6) is based on the solution of the normal equation associated with Eq. (25), namely

$$\mathscr{K}^*(\mathscr{K}\boldsymbol{\eta}) = \mathscr{K}^*\mathbf{y}, \tag{26}$$

and this is equivalent to minimizing the residual functional

$$\mathscr{F}_1 : L^2(\Gamma_1)^d \to [0, \infty), \qquad \mathscr{F}_1(\boldsymbol{\eta}) = \|\mathscr{K}\boldsymbol{\eta} - \mathbf{y}\|_{L^2(\Gamma_0)^d}. \tag{27}$$

On using Lemma 1 for the definition of the adjoint operator, $\mathscr{K}^*$, the following convergent algorithm is obtained, see also Marin et al. (2002b).

Step 1. Set $k = 1$ and choose an arbitrary function $\boldsymbol{\eta}^{(k)} \in L^2(\Gamma_1)^d$.
Step 2. Solve the direct problem

$$\begin{cases} \mathscr{L}\mathbf{u}^{(k)}(\mathbf{x}) = \mathbf{0}, & \mathbf{x} \in \Omega, \\ \mathscr{N}\mathbf{u}^{(k)}(\mathbf{x}) \equiv \boldsymbol{\sigma}(\mathbf{u}^{(k)}(\mathbf{x})) \cdot \mathbf{n}(\mathbf{x}) = \boldsymbol{\psi}(\mathbf{x}), & \mathbf{x} \in \Gamma_0, \\ \mathbf{u}^{(k)}(\mathbf{x}) = \boldsymbol{\eta}^{(k)}(\mathbf{x}), & \mathbf{x} \in \Gamma_1, \end{cases} \tag{28}$$

to determine $\mathbf{u}^{(k)}(\mathbf{x})$, $\mathbf{x} \in \Omega$, and $\mathscr{N}\mathbf{u}^{(k)}(\mathbf{x}) \equiv \mathbf{t}^{(k)}(\mathbf{x})$, $\mathbf{x} \in \Gamma_1$. Set

$$\boldsymbol{\xi}^{(k)}(\mathbf{x}) = \boldsymbol{\varphi}(\mathbf{x}) - \mathbf{u}^{(k)}(\mathbf{x}), \qquad \mathbf{x} \in \Gamma_0. \tag{29}$$

Step 3. Solve the adjoint problem

$$\begin{cases} \mathscr{L}^*\mathbf{v}^{(k)}(\mathbf{x}) = \mathbf{0}, & \mathbf{x} \in \Omega, \\ \mathscr{N}^*\mathbf{v}^{(k)}(\mathbf{x}) \equiv \boldsymbol{\sigma}(\mathbf{v}^{(k)}(\mathbf{x})) \cdot \mathbf{n}(\mathbf{x}) = \boldsymbol{\xi}^{(k)}(\mathbf{x}), & \mathbf{x} \in \Gamma_0, \\ \mathbf{v}^{(k)}(\mathbf{x}) = \mathbf{0}, & \mathbf{x} \in \Gamma_1, \end{cases} \tag{30}$$

to determine

$$\alpha_{k-1} = \begin{cases} 0 & \text{if } k = 1, \\ \|\mathscr{N}^*\mathbf{v}^{(k)}\|_{L^2(\Gamma_1)^d}^2 / \|\mathscr{N}^*\mathbf{v}^{(k-1)}\|_{L^2(\Gamma_1)^d}^2 & \text{if } k > 1, \end{cases} \tag{31}$$

$$\boldsymbol{\zeta}^{(k)}(\mathbf{x}) = \begin{cases} -\mathscr{N}^*\mathbf{v}^{(k)}(\mathbf{x}), & \mathbf{x} \in \Gamma_1 \text{ if } k = 1, \\ -\mathscr{N}^*\mathbf{v}^{(k)}(\mathbf{x}) + \alpha_{k-1}\boldsymbol{\zeta}^{(k-1)}(\mathbf{x}), & \mathbf{x} \in \Gamma_1 \text{ if } k > 1. \end{cases} \tag{32}$$

Step 4. Solve the direct problem

$$\begin{cases} \mathscr{L}\mathbf{w}^{(k)}(\mathbf{x}) = \mathbf{0}, & \mathbf{x} \in \Omega, \\ \mathscr{N}\mathbf{w}^{(k)}(\mathbf{x}) \equiv \boldsymbol{\sigma}(\mathbf{w}^{(k)}(\mathbf{x})) \cdot \mathbf{n}(\mathbf{x}) = \mathbf{0}, & \mathbf{x} \in \Gamma_0, \\ \mathbf{w}^{(k)}(\mathbf{x}) = \boldsymbol{\zeta}^{(k)}(\mathbf{x}), & \mathbf{x} \in \Gamma_1, \end{cases} \tag{33}$$

to determine

$$\beta_k = \|\mathscr{N}^*\mathbf{v}^{(k)}\|_{L^2(\Gamma_1)^d}^2 / \|\mathbf{w}^{(k)}\|_{L^2(\Gamma_0)^d}^2, \tag{34}$$

$$\boldsymbol{\eta}^{(k+1)}(\mathbf{x}) = \boldsymbol{\xi}^{(k)}(\mathbf{x}) + \beta_k \boldsymbol{\zeta}^{(k)}(\mathbf{x}), \qquad \mathbf{x} \in \Gamma_1. \tag{35}$$

Step 5. Set $k = k + 1$ and repeat Steps 2–4 until a prescribed stopping criterion is satisfied.

It is worth mentioning that the CGM has been implemented for solving numerically the Cauchy problem associated with several partial differential operators, such as the heat equation by Háo and Reinhardt (1998) and Bastay et al. (2001), the Laplace equation by Háo and Lesnic (2000), the Lamé system of linear elasticity by Marin et al. (2002b), Helmholtz-type equations by Marin et al. (2003) and the Stokes system in hydrostatics by Johansson and Lesnic (2006a).

4.2. The minimal error method

The MEM is a variant of the CGM, see King (1989), that minimizes the iteration error functional

$$\mathscr{F}_2 : L^2(\Gamma_1)^d \to [0, \infty), \qquad \mathscr{F}_2(\boldsymbol{\eta}) = \|\boldsymbol{\eta} - \mathscr{K}^{-1}\mathbf{y}\|_{L^2(\Gamma_1)^d}, \tag{36}$$

instead of the residual functional $\mathscr{F}_1$ given by Eq. (27). On using Lemma 1 for the definition of the adjoint operator, $\mathscr{K}^*$, and the algorithm of Hanke (1995a) for the Cauchy problem in linear elasticity (6), the following convergent algorithm is obtained:

Step 1. Set $k = 1$ and choose an arbitrary function $\boldsymbol{\eta}^{(k)} \in L^2(\Gamma_1)^d$.
Step 2. Solve the direct problem

$$\begin{cases} \mathscr{L}\mathbf{u}^{(k)}(\mathbf{x}) = \mathbf{0}, & \mathbf{x} \in \Omega, \\ \mathscr{N}\mathbf{u}^{(k)}(\mathbf{x}) \equiv \boldsymbol{\sigma}(\mathbf{u}^{(k)}(\mathbf{x})) \cdot \mathbf{n}(\mathbf{x}) = \boldsymbol{\psi}(\mathbf{x}), & \mathbf{x} \in \Gamma_0, \\ \mathbf{u}^{(k)}(\mathbf{x}) = \boldsymbol{\eta}^{(k)}(\mathbf{x}), & \mathbf{x} \in \Gamma_1, \end{cases} \tag{37}$$

to determine $\mathbf{u}^{(k)}(\mathbf{x})$, $\mathbf{x} \in \Omega$, and $\mathscr{N}\mathbf{u}^{(k)}(\mathbf{x}) \equiv \mathbf{t}^{(k)}(\mathbf{x})$, $\mathbf{x} \in \Gamma_1$. Set

$$\boldsymbol{\xi}^{(k)}(\mathbf{x}) = \boldsymbol{\varphi}(\mathbf{x}) - \mathbf{u}^{(k)}(\mathbf{x}), \qquad \mathbf{x} \in \Gamma_0. \tag{38}$$

Step 3. Solve the adjoint problem

$$\begin{cases} \mathscr{L}^* \mathbf{v}^{(k)}(\mathbf{x}) = \mathbf{0}, & \mathbf{x} \in \Omega, \\ \mathscr{N}^* \mathbf{v}^{(k)}(\mathbf{x}) \equiv \boldsymbol{\sigma}(\mathbf{v}^{(k)}(\mathbf{x})) \cdot \mathbf{n}(\mathbf{x}) = \boldsymbol{\xi}^{(k)}(\mathbf{x}), & \mathbf{x} \in \Gamma_0, \\ \mathbf{v}^{(k)}(\mathbf{x}) = \mathbf{0}, & \mathbf{x} \in \Gamma_1, \end{cases} \tag{39}$$

to determine

$$\gamma_{k-1} = \begin{cases} 0 & \text{if } k = 1, \\ \|\boldsymbol{\xi}^{(k)}\|^2_{L^2(\Gamma_0)^d} / \|\boldsymbol{\xi}^{(k-1)}\|^2_{L^2(\Gamma_0)^d} & \text{if } k > 1, \end{cases} \tag{40}$$

$$\zeta^{(k)}(\mathbf{x}) = \begin{cases} -\mathscr{N}^* \mathbf{v}^{(k)}(\mathbf{x}), & \mathbf{x} \in \Gamma_1 \quad \text{if } k = 1, \\ -\mathscr{N}^* \mathbf{v}^{(k)}(\mathbf{x}) + \gamma_{k-1} \zeta^{(k-1)}(\mathbf{x}), & \mathbf{x} \in \Gamma_1 \quad \text{if } k > 1, \end{cases} \tag{41}$$

$$\delta_k = \|\boldsymbol{\xi}^{(k)}\|^2_{L^2(\Gamma_0)^d} / \|\zeta^{(k)}\|^2_{L^2(\Gamma_1)^d}, \tag{42}$$

$$\boldsymbol{\eta}^{(k+1)}(\mathbf{x}) = \boldsymbol{\eta}^{(k)}(\mathbf{x}) + \delta_k \zeta^{(k)}(\mathbf{x}), \qquad \mathbf{x} \in \Gamma_1. \tag{43}$$

Step 4. Set $k = k + 1$ and repeat Steps 2 and 3 until a prescribed stopping criterion is satisfied.

It should be mentioned that the MEM has recently been implemented for solving numerically the Cauchy problem associated with the Stokes system in hydrostatics by Johansson and Lesnic (2006b). To our knowledge, the MEM has never been applied to obtaining the numerical solution of the Cauchy problem in linear elasticity.

5. Numerical results and discussion

It is the purpose of this section to present the numerical implementation of the MEM using the BEM in the case of two-dimensional isotropic linear elastic materials and analyse the numerical convergence and stability of this procedure. Moreover, a comparison of this iterative method with the CGM and LFM previously investigated by Marin et al. (2002b) and Marin and Lesnic (2005), respectively, is also performed.

5.1. Examples

In order to present the performance of the aforementioned iterative methods, we consider a two-dimensional isotropic linear elastic medium characterized by the material constants $G = 3.35 \times 10^{10}$ N/m^2 and $v = 0.34$ corresponding to a copper alloy and we solve the Cauchy problem (6) for two situations in a smooth, doubly connected geometry. More precisely, we consider the following analytical solution for the displacements:

$$u_i^{(an)}(x_1, x_2) = \frac{1}{2G(1+v)} \left(V(1-v)x_i - W(1+v)\frac{x_i}{x_1^2 + x_2^2} \right) x_i, \qquad i = 1, 2, \tag{44}$$

where

$$V = -\frac{\sigma_{out} r_{out}^2 - \sigma_{int} r_{int}^2}{r_{out}^2 - r_{int}^2}, \quad W = \frac{(\sigma_{out} - \sigma_{int}) r_{out}^2 r_{int}^2}{r_{out}^2 - r_{int}^2}, \quad \sigma_{int} = 1.0 \times 10^{10} \text{ N/m}^2, \quad \sigma_{out} = 2.0 \times 10^{10} \text{ N/m}^2, \tag{45}$$

in the annular domain $\Omega = \{\mathbf{x} = (x_1, x_2) | r_{int}^2 < x_1^2 + x_2^2 < r_{out}^2 \}$, where $r_{int} = 1$ and $r_{out} = 4$, which corresponds to constant internal and external pressures for which the stress tensor is given by

$$\sigma_{11}^{(an)}(x_1, x_2) = V + W \frac{x_1^2 - x_2^2}{(x_1^2 + x_2^2)^2}, \quad \sigma_{22}^{(an)}(x_1, x_2) = V - W \frac{x_1^2 - x_2^2}{(x_1^2 + x_2^2)^2}, \quad \sigma_{12}^{(an)}(x_1, x_2) = \sigma_{21}^{(an)}(x_1, x_2) = 2W \frac{x_1 x_2}{(x_1^2 + x_2^2)^2}. \tag{46}$$

Problem I. Consider $\Gamma_0 = \Gamma_{out} = \{\mathbf{x} \in \Gamma | \rho(\mathbf{x}) = r_{out}\}$ and $\Gamma_1 = \Gamma_{int} = \{\mathbf{x} \in \Gamma | \rho(\mathbf{x}) = r_{int}\}$, where $\rho(\mathbf{x})$ is the radial polar coordinate of $\mathbf{x}$.

Problem II. Consider $\Gamma_0 = \Gamma_{int} = \{\mathbf{x} \in \Gamma | \rho(\mathbf{x}) = r_{int}\}$ and $\Gamma_1 = \Gamma_{out} = \{\mathbf{x} \in \Gamma | \rho(\mathbf{x}) = r_{out}\}$.

Moreover, in order to present the limitations of the proposed numerical method, we also analyse an additional severe inverse problem. More precisely, we investigate a Cauchy problem for which the traction data to be reconstructed on the under-specified boundary are discontinuous. We consider the same two-dimensional geometry and isotropic linear elastic material as those corresponding to Problems I and II, and the following tractions on the boundary $\Gamma = \Gamma_0 \cup \Gamma_1$:

$$t_1^{(an)}(\mathbf{x}) = t_2^{(an)}(\mathbf{x}) = 0, \qquad \mathbf{x} \in \Gamma_0 \tag{47}$$

$$t_1^{(an)}(\mathbf{x}) = \begin{cases} \sigma_1 n_1(\mathbf{x}), & \mathbf{x} \in \Gamma_1 : \theta(\mathbf{x}) \in [0, \theta_0] \cup [\pi - \theta_0, \pi + \theta_0] \cup [2\pi - \theta_0, 2\pi), \\ 0, & \mathbf{x} \in \Gamma_1 : \theta(\mathbf{x}) \in (\theta_0, \pi - \theta_0) \cup (\pi + \theta_0, 2\pi - \theta_0), \end{cases} \tag{48}$$

$$t_2^{(an)}(\mathbf{x}) = \begin{cases} 0, & \mathbf{x} \in \Gamma_1 : \theta(\mathbf{x}) \in [0, \theta_0] \cup [\pi - \theta_0, \pi + \theta_0] \cup [2\pi - \theta_0, 2\pi), \\ \sigma_2 n_2(\mathbf{x}), & \mathbf{x} \in \Gamma_1 : \theta(\mathbf{x}) \in (\theta_0, \pi - \theta_0) \cup (\pi + \theta_0, 2\pi - \theta_0), \end{cases} \tag{49}$$

where $\sigma_1 = \sigma_2 = 1.0 \times 10^{10}$ N/m^2, $\theta(\mathbf{x})$ is the polar coordinate of $\mathbf{x}$ and $\theta_0 = \pi/4$. It should be mentioned that the corresponding analytical expressions for the displacements $u_i^{(an)}(\mathbf{x})$, $i = 1, 2$, are not available in this case, but they can be obtained numerically by solving the following Neumann problem:

$$\begin{cases} \mathscr{L}\mathbf{u}(\mathbf{x}) = \mathbf{0}, & \mathbf{x} \in \Omega, \\ \mathscr{N}\mathbf{u}(\mathbf{x}) = \mathbf{t}^{(an)}(\mathbf{x}), & \mathbf{x} \in \Gamma_0 \cup \Gamma_1, \end{cases} \tag{50}$$

where the rigid body displacements are eliminated by using

$$\int_\Gamma \mathbf{u}(\mathbf{x}) d\Omega(\mathbf{x}) = \mathbf{0}, \qquad \int_\Gamma \mathbf{u}(\mathbf{x}) \times \mathbf{x} d\Omega(\mathbf{x}) = \mathbf{0}. \tag{51}$$

Problem III. Hence the last Cauchy problem investigated is given by $\Gamma_0 = \Gamma_{out} = \{\mathbf{x} \in \Gamma | \rho(\mathbf{x}) = r_{out}\}$ and $\Gamma_1 = \Gamma_{int} = \{\mathbf{x} \in \Gamma | \rho(\mathbf{x}) = r_{int}\}$, in which $t_i^{(an)}(\mathbf{x})$, $i = 1, 2$, are described by Eqs. (47)–(49), whilst $u_i^{(an)}(\mathbf{x})$, $i = 1, 2$, are retrieved by solving the Neumann problem (50).

5.2. The boundary element method

In this section, we describe the BEM for homogeneous isotropic linear elastic materials in two-dimensions, i.e. $d = 2$, although similar arguments apply for homogeneous anisotropic linear elastic materials, as well as in higher dimensions, i.e. $d > 2$. The Lamé system (1) in the two-dimensional case can be formulated in integral form with the aid of the Second Theorem of Betti, see e.g. Landau and Lifshits (1986), namely

$$c_{ij}(\mathbf{x}) u_j(\mathbf{x}) + \oint_\Gamma T_{ij}(\mathbf{y}, \mathbf{x}) u_j(\mathbf{y}) d\Gamma(\mathbf{y}) = \int_\Gamma U_{ij}(\mathbf{y}, \mathbf{x}) t_j(\mathbf{y}) d\Gamma(\mathbf{y}) \tag{52}$$

for $i, j = 1, 2$, $\mathbf{x} \in \overline{\Omega}$, and $\mathbf{y} \in \Gamma$, where the first integral is taken in the sense of the Cauchy principal value, $c_{ij}(\mathbf{x}) = 1$ for $\mathbf{x} \in \Omega$ and $c_{ij}(\mathbf{x}) = 1/2$ for $\mathbf{x} \in \Gamma$ (smooth), and U_{ij} and T_{ij} are the fundamental displacements and tractions for the two-dimensional isotropic linear elasticity given by

$$U_{ij}(\mathbf{y}, \mathbf{x}) = C_1 \left(C_2 \delta_{ij} \ln r(\mathbf{y}, \mathbf{x}) - \frac{\partial r(\mathbf{y}, \mathbf{x})}{\partial y_i} \frac{\partial r(\mathbf{y}, \mathbf{x})}{\partial y_j} \right) \tag{53}$$

and

$$T_{ij}(\mathbf{y}, \mathbf{x}) = \frac{C_3}{r(\mathbf{y}, \mathbf{x})} \left[\left(C_4 \delta_{ij} + 2 \frac{\partial r(\mathbf{y}, \mathbf{x})}{\partial y_i} \frac{\partial r(\mathbf{y}, \mathbf{x})}{\partial y_j} \right) \frac{\partial r(\mathbf{y}, \mathbf{x})}{\partial n(\mathbf{y})} - C_4 \left(\frac{\partial r(\mathbf{y}, \mathbf{x})}{\partial y_i} n_j(\mathbf{y}) - \frac{\partial r(\mathbf{y}, \mathbf{x})}{\partial y_j} n_i(\mathbf{y}) \right) \right], \tag{54}$$

respectively. Here, r$(\mathbf{y}, \mathbf{x})$ represents the distance between the node/collocation point $\mathbf{x}$ and the field point $\mathbf{y}$, whilst the constants C_1, C_2, C_3 and C_4 are given by

$$C_1 = -1/[8\pi G(1 - \overline{v})], \qquad C_2 = 3 - 4\overline{v}, \qquad C_3 = -1/[4\pi(1 - \overline{v})], \qquad C_4 = 1 - 2\overline{v}, \tag{55}$$

where $\overline{v} = v$ for the plane strain state and $\overline{v} = v/(1 + v)$ for the plane stress state.

A BEM with continuous linear boundary elements, see e.g. Brebbia et al. (1984), is employed in order to discretise the integral equation (52). If the boundaries Γ_{int} and Γ_{out} are discretised into N_{int} and N_{out} continuous linear boundary elements, respectively, such that $N = N_{int} + N_{out}$, then on applying the boundary integral equation (52) at each node/collocation point, we arrive at the following system of linear algebraic equations:

$$\mathbf{AU} = \mathbf{BT}. \tag{56}$$

Here, $\mathbf{A}$ and $\mathbf{B}$ are matrices which depend solely on the geometry of the boundary Γ and material properties, i.e. the Poisson ratio, v, and the shear modulus, G, and can be calculated analytically, and the vectors $\mathbf{U}$ and $\mathbf{T}$ consist of the discretised values of the boundary displacements and tractions, respectively.

For the inverse problems considered in this study, the BEM system of linear algebraic equations (56) has been solved for each of the well-posed, direct and adjoint problems that occur at each iteration, k, of the LFM, CGM and MEM presented in Sections 3.3, 4.1 and 4.2, respectively, to provide simultaneously the unspecified boundary displacements and tractions on Γ_1. The number of continuous linear boundary elements used for discretising the boundary Γ was taken to be $N \in \{60, 120, 240\}$ such that $N_{out} = N_{int}/2 = N/3$. It is also important to mention that for the inverse problems investigated in this paper, as well as all iterative methods analysed herein, the initial guess, $\boldsymbol{\eta}^{(1)}$, for the displacement vector on the under-specified boundary, $\mathbf{u}|_{\Gamma_1}$, was taken to be

$$\boldsymbol{\eta}^{(1)}(\mathbf{x}) = \mathbf{0}, \qquad \mathbf{x} \in \Gamma_1. \tag{57}$$

5.3. Convergence of the MEM

In order to investigate the convergence of the algorithm, at every iteration, k, we evaluate the accuracy errors defined by

$$e_{\mathbf{u}}^{a}(k) = \|\mathbf{u}^{(k)} - \mathbf{u}^{(an)}\|_{L^2(\Gamma_1)^d} = \|\boldsymbol{\eta}^{(k)} - \mathbf{u}^{(an)}\|_{L^2(\Gamma_1)^d} \tag{58}$$

and

$$e_{\mathbf{t}}^{a}(k) = \|\mathbf{t}^{(k)} - \mathbf{t}^{(an)}\|_{L^2(\Gamma_1)^d} = \|\mathcal{N}\mathbf{u}^{(k)} - \mathbf{t}^{(an)}\|_{L^2(\Gamma_1)^d}, \tag{59}$$

where $\mathbf{u}^{(k)}$ and $\mathbf{t}^{(k)}$ are the displacement and the traction vectors on the boundary Γ_1 retrieved after k iterations, respectively. The error in predicting the displacement vector inside the solution domain Ω may also be evaluated by using the expression

$$E_{\mathbf{u}}^{a}(k) = \|\mathbf{u}^{(k)} - \mathbf{u}^{(an)}\|_{L^2(\Omega_1)^d} \tag{60}$$

However, this is not pursued here since the error $E_{\mathbf{u}}^{a}$ has a similar evolution to that of the errors $e_{\mathbf{u}}^{a}$ and $e_{\mathbf{t}}^{a}$, as at each iteration the values of the displacement vector inside the solution domain Ω are retrieved from the values of the displacement, $\mathbf{u}$, and traction, $\mathbf{t}$, vectors on Γ.

Fig. 1 shows, on a logarithmic scale, the accuracy errors $e_{\mathbf{u}}^{a}$ and $e_{\mathbf{t}}^{a}$ as functions of the number of iterations, k, obtained for Problem I with $N \in \{60, 120, 240\}$ when using "exact" boundary data for the inverse problem, i.e. boundary data obtained by solving a direct, well-posed problem, namely

$$\begin{cases} \mathscr{L}\mathbf{u}(\mathbf{x}) = \mathbf{0}, & \mathbf{x} \in \Omega, \\ \mathbf{u}(\mathbf{x}) = \mathbf{u}^{(an)}(\mathbf{x}), & \mathbf{x} \in \Gamma_0, \\ \mathscr{N}\mathbf{u}(\mathbf{x}) = \mathbf{t}^{(an)}(\mathbf{x}), & \mathbf{x} \in \Gamma_1. \end{cases} \tag{61}$$

It can be seen from this figure that, for all discretisations used in this paper, both errors $e_{\mathbf{u}}^{a}$ and $e_{\mathbf{t}}^{a}$ keep decreasing until around $k = 8$ iterations, after which the convergence rate of the aforementioned accuracy errors becomes very slow so that they reach a plateau. As expected, for each of the BEM discretisations employed, $e_{\mathbf{u}}^{a}(k) < e_{\mathbf{t}}^{a}(k)$ for all $k > 0$, i.e. displacements are more accurate than tractions, and the finer the BEM mesh, the more accurate the numerical results for both displacement and traction vectors, i.e. the MEM is convergent with respect to refining the mesh size. Furthermore, as N increases, the errors $e_{\mathbf{u}}^{a}$ and $e_{\mathbf{t}}^{a}$ decrease showing that $N \geqslant 120$ ensures a sufficient discretisation for the accuracy to be achieved.

The same conclusion can be drawn from Fig. 2(a) and (b), which illustrate the analytical and numerical displacements u_1 and u_2, respectively, obtained on the under-specified boundary Γ_1 after $k = 1000$ iterations, for $N \in \{60, 120, 240\}$, and Fig. 2(c) and (d), which present graphically the corresponding analytical and numerical values for the tractions t_1 and t_2, respectively. From Figs. 1 and 2, it can be concluded that the MEM described in Section 4.2 is convergent with respect to increasing the number of iterations, k, as well as refining the BEM mesh size, provided that exact boundary data are prescribed on Γ_0. Although not presented, it should be mentioned that similar results have been obtained for Problems II and III.
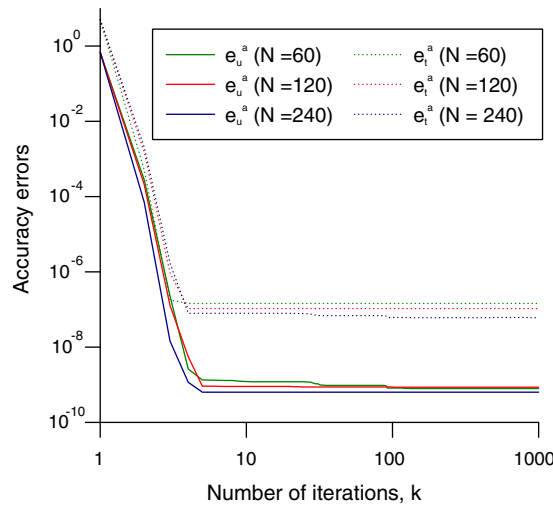
Fig. 1. The accuracy errors $e_{\mathbf{u}}^{a}$ (——), and $e_{\mathbf{t}}^{a}$ (· · ·), as functions of the number of iterations, k, obtained using the MEM, exact Cauchy data and various numbers of continuous linear boundary elements, namely $N \in \{60, 120, 240\}$, for Problem I.

Fig. 2. The analytical and numerical displacements (a) u_1, and (b) u_2, and the analytical and numerical tractions (c) t_1, and (d) t_2, obtained on the under-specified boundary $\Gamma_1 \equiv \Gamma_{\text{int}}$ using the MEM, exact Cauchy data and various numbers of continuous linear boundary elements, namely $N \in \{60, 120, 240\}$, for Problem I.
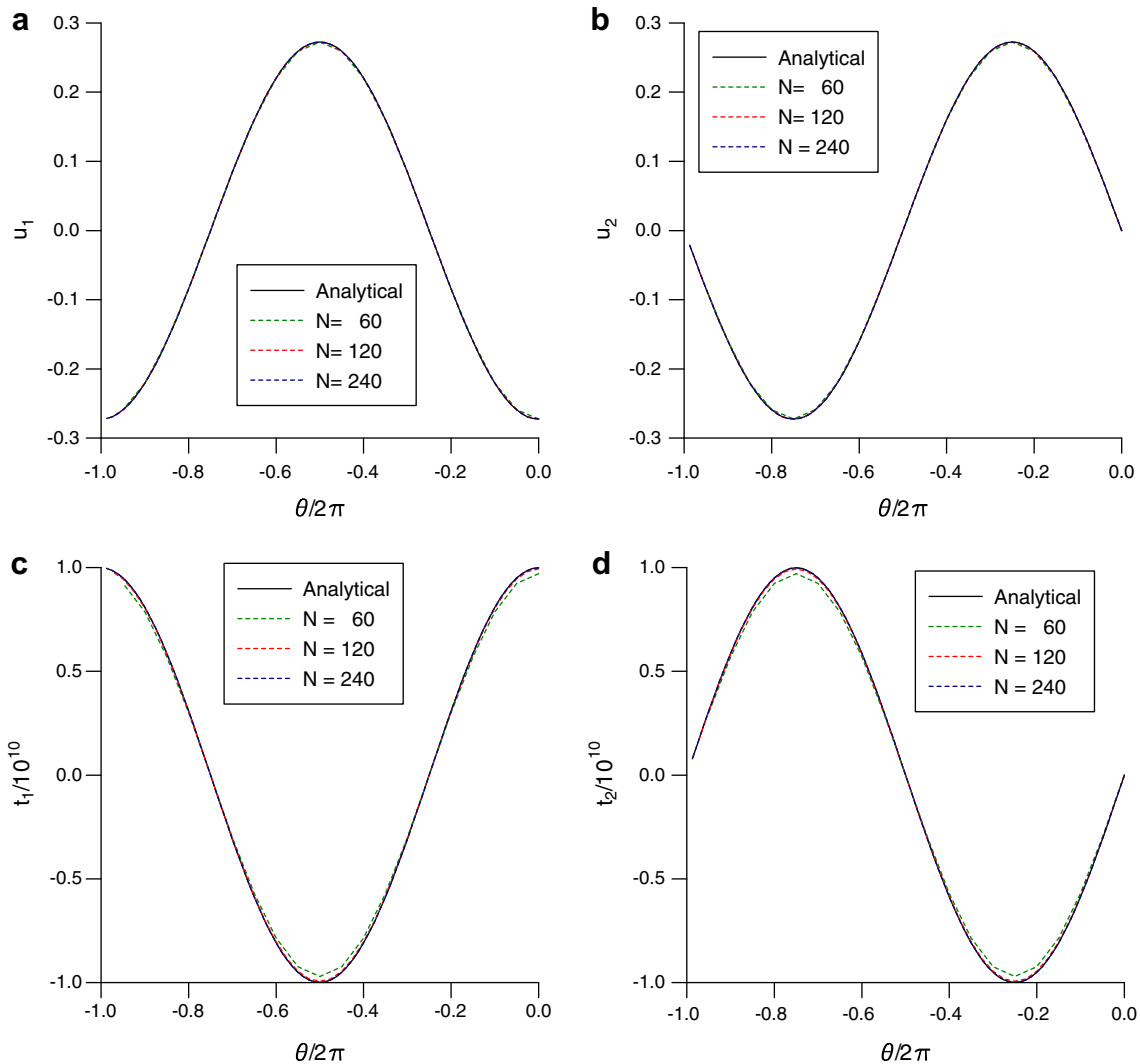
5.4. Regularizing stopping criteria

Once the convergence with respect to increasing N of the numerical solution to the exact solution has been established, we fix $N = 240$, i.e. $N_{\text{out}}/2 = N_{\text{int}} = 80$, and investigate the stability of the numerical solution for the examples considered. To do so and in order to simulate the inherent inaccuracies in the measured data on Γ_0, we assume that various levels of Gaussian random noise, $p_{\mathbf{u}}$, have been added into the exact displacement data $\mathbf{u}|_{\Gamma_0} = \boldsymbol{\varphi}$, so that the following perturbed displacements are available:

$$\boldsymbol{\varphi}^\varepsilon \in L^2(\Gamma_0)^d : \quad \|\mathbf{u}^{(\text{an})}|_{\Gamma_0} - \boldsymbol{\varphi}^\varepsilon\|_{L^2(\Gamma_0)^d} = \varepsilon. \tag{62}$$

Fig. 3(a) and (b) present the accuracy errors $e_{\mathbf{u}}^{\text{a}}$ and $e_{\mathbf{t}}^{\text{a}}$, respectively, as functions of the number of iterations, k, obtained for $p_u \in \{1, 3, 5\}\%$ in the case of Problem I. From these figures it can be seen that as $p_{\mathbf{u}}$ decreases then $e_{\mathbf{u}}^{\text{a}}$ and $e_{\mathbf{t}}^{\text{a}}$ decrease. However, the errors in predicting the displacement and traction vectors on the under-specified boundary Γ_1 decrease up to a certain iteration number and after that they start increasing. If the iterative process is continued beyond this point then the numerical solutions lose their smoothness and become highly oscillatory and unbounded, i.e. unstable. Therefore, a regularizing stopping criterion must be used in order to terminate the iterative process at the point where the errors in the numerical solutions start increasing.

To define the stopping criteria required for regularizing/stabilizing the iterative methods analysed in this paper, the following two convergence errors are introduced:

$$e_{\mathbf{u}}^c(k) = \|\mathbf{u}^{(k)}|_{\Gamma_0} - \boldsymbol{\varphi}^{\varepsilon}\|_{L^2(\Gamma_0)^d} \tag{63}$$

and

$$E_c(k) = \left(\sum_{j=1}^{k} e_{\mathbf{u}}^c(j)^{-2} \right)^{-1/2}, \tag{64}$$

respectively. In the case of the CGM and LFM, the iterative process is ceased according to the discrepancy principle of Morozov (1966), see also Marin et al. (2002b) and Marin and Lesnic (2005), namely at the optimal iteration number, k_{opt}, given by

$$k_{opt} = \min_{k \in \mathbb{Z}, k>0} \{ e_{\mathbf{u}}^c(k) \leqslant \tau\varepsilon \}, \tag{65}$$

where $\tau > 1$ is some fixed constant. It is worth mentioning the fact that, according to Nemirovskii (1986), the stopping criterion (65) is an order optimal stopping rule for the CGM. Since it was previously shown by Hanke (1995b) that the discrepancy principle (65) is not a regularizing stopping rule for the MEM, then based on the convergence error, E_c, given by Eq. (64), the iterative process is ceased in this case at the following optimal iteration number:

$$k_{opt} = \min_{k \in \mathbb{Z}, k>0} \{ E_c(k) \leqslant \tau\varepsilon \}, \tag{66}$$

where $\tau > 1$ is some fixed constant.

Fig. 3(c) presents the evolution of the convergence error E_c with respect to the number of iterations performed, k, using various levels of Gaussian noise added into the displacements on the over-specified boundary Γ_0, namely $p_{\mathbf{u}} \in \{1\%, 3\%, 5\%\}$,
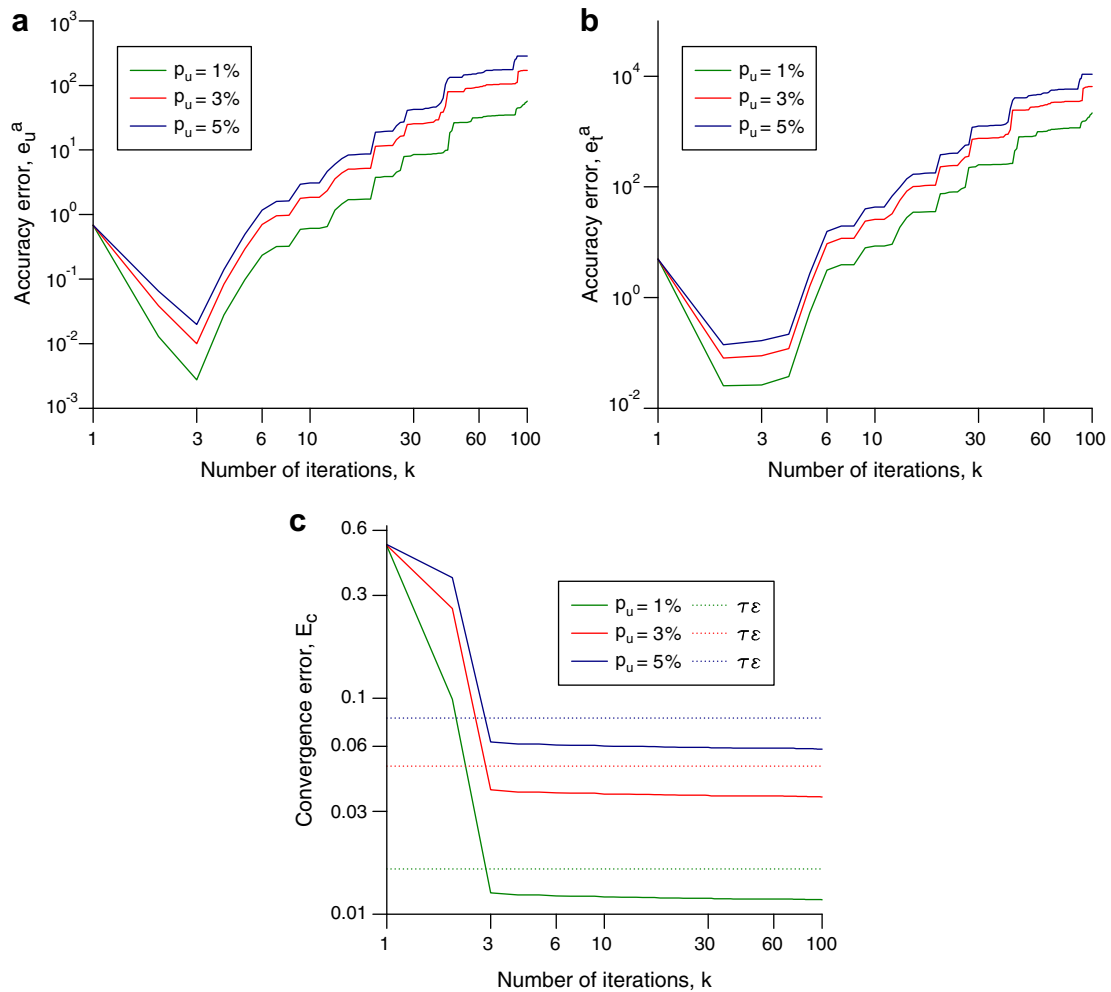

Fig. 3. The accuracy errors (a) $e_{\mathbf{u}}^a$, (b) e_t^a, and (c) convergence error, E_c, as functions of the number of iterations, k, obtained using the MEM, the stopping criterion given by Eq. (66) and various amounts of noise added into the displacement, $\mathbf{u}|_{\Gamma_0} \equiv \mathbf{u}|_{\Gamma_{out}}$, i.e. $p_{\mathbf{u}} \in \{1\%, 3\%, 5\%\}$, for Problem I.

and $\tau \approx 1.35$ in the stopping criterion (66), for Problem I. By comparing Fig. 3(a)–(c), it can be seen that selecting the optimal iteration number, k_{opt}, according to the stopping rule given by Eq. (66) captures very well the minimum values for the accuracy errors e_u^a and e_t^a; therefore, Eq. (66) represents a stabilizing stopping criterion for the MEM. Although not illustrated, it is important to mention that similar results and conclusions have been obtained for Problems II and III.

As mentioned in the previous section, for exact data the iterative process is convergent with respect to increasing the number of iterations, k, since the accuracy errors e_u^a and e_t^a keep decreasing even after a large number of iterations, see Fig. 1. It should be noted in this case that a stopping criterion is not necessary since the numerical solution is convergent with respect to increasing the number of iterations. However, even in this case E_c, e_u^a and e_t^a have a similar behaviour and the error E_c may be used to stop the iterative process at the point where the rate of convergence is very small and no substantial improvement in the numerical solution is obtained even if the iterative process is continued. Therefore, it can be concluded that the regularizing stopping criterion proposed for the MEM is very efficient in locating the point where the errors start increasing and the iterative process should be ceased.

5.5. Stability of the MEM

Although for the LFM and CGM the choice of τ close to unity results in accurate and stable results for the displacement and traction vectors on the under-specified boundary Γ_1, in the case of the MEM values for τ between 1.0 and 1.1 produce numerical results exhibiting a slightly oscillatory unstable behaviour for the aforementioned vectors. Consequently, this study shows that the MEM is more sensitive to the choice of τ than in the other iterative methods, as something expected

Fig. 4. The analytical and numerical displacements (a) u_1, and (b) u_2, and the analytical and numerical tractions (c) t_1, and (d) t_2, obtained on the under-specified boundary $\Gamma_1 \equiv \Gamma_{int}$ using the MEM, the stopping criterion given by Eq. (66) and various amounts of noise added into the displacement, $\mathbf{u}|_{\Gamma_0} \equiv \mathbf{u}|_{\Gamma_{out}}$, i.e. $p_{\mathbf{u}} \in \{1\%, 3\%, 5\%\}$, for Problem I.

from the preliminary investigation of King (1989) and also in accordance with the recent results of Johansson and Lesnic (2006b). Also, it should be mentioned that a value of $\tau \approx 1.35$ was found to be optimal for the MEM for all levels of noise, as well as the inverse problems investigated in this paper, as reported by Johansson and Lesnic (2006b) for the Stokes system in hydrostatic.

Based on the stopping criterion (66) described in Section 5.4, the numerical results obtained for the x_1- and x_2-components of the displacement vector obtained on the under-specified boundary $\Gamma_1 \equiv \Gamma_{\text{int}}$ and their corresponding analytical values are presented in Fig. 4(a) and (b), respectively, for various amounts of noise added into the displacement, $\mathbf{u}|_{\Gamma_0} \equiv \mathbf{u}|_{\Gamma_{\text{out}}}$, i.e. $p_{\mathbf{u}} \in \{1\%, 3\%, 5\%\}$, in the case of Problem I. The associated analytical and numerical values for t_1 and t_2, retrieved on Γ_1 using the MEM and the stopping criterion (66), are illustrated in Fig. 4(c) and (d), respectively. From these figures it can be seen that the numerical solution, for both the displacement and traction vectors, is a stable approximation to the corresponding exact solution, free of unbounded and rapid oscillations, and it converges to the exact solution as the level of noise, $p_{\mathbf{u}}$, added into the input boundary data decreases.

The same conclusion can be drawn from Fig. 5(a)–(d) which present the numerical values for the displacement and traction vectors, in comparison with their analytical counterparts, obtained on the under-specified boundary $\Gamma_1 \equiv \Gamma_{\text{out}}$ using the MEM, the regularizing stopping criterion (66) and various amounts of noise added into the displacement, $\mathbf{u}|_{\Gamma_0} \equiv \mathbf{u}|_{\Gamma_{\text{int}}}$, i.e. $p_{\mathbf{u}} \in \{1\%, 5\%, 10\%\}$, for Problem II. It is important to mention that, as expected, Problem I is more sensitive to noise added into the boundary displacement data than Problem II. A possible explanation for this might be given by the relation between the lengths of the inner and outer boundaries, Γ_{int} and Γ_{out}, on which perturbed Dirichlet data are available, in the sense that $\text{meas}(\Gamma_{\text{int}}) < \text{meas}(\Gamma_{\text{out}})$.

The limitations of the proposed MEM are very well emphasized by the numerical results obtained for Problem III and illustrated in Fig. 6(a)–(d). More precisely, in this case discontinuous Neumann boundary conditions have to be recovered
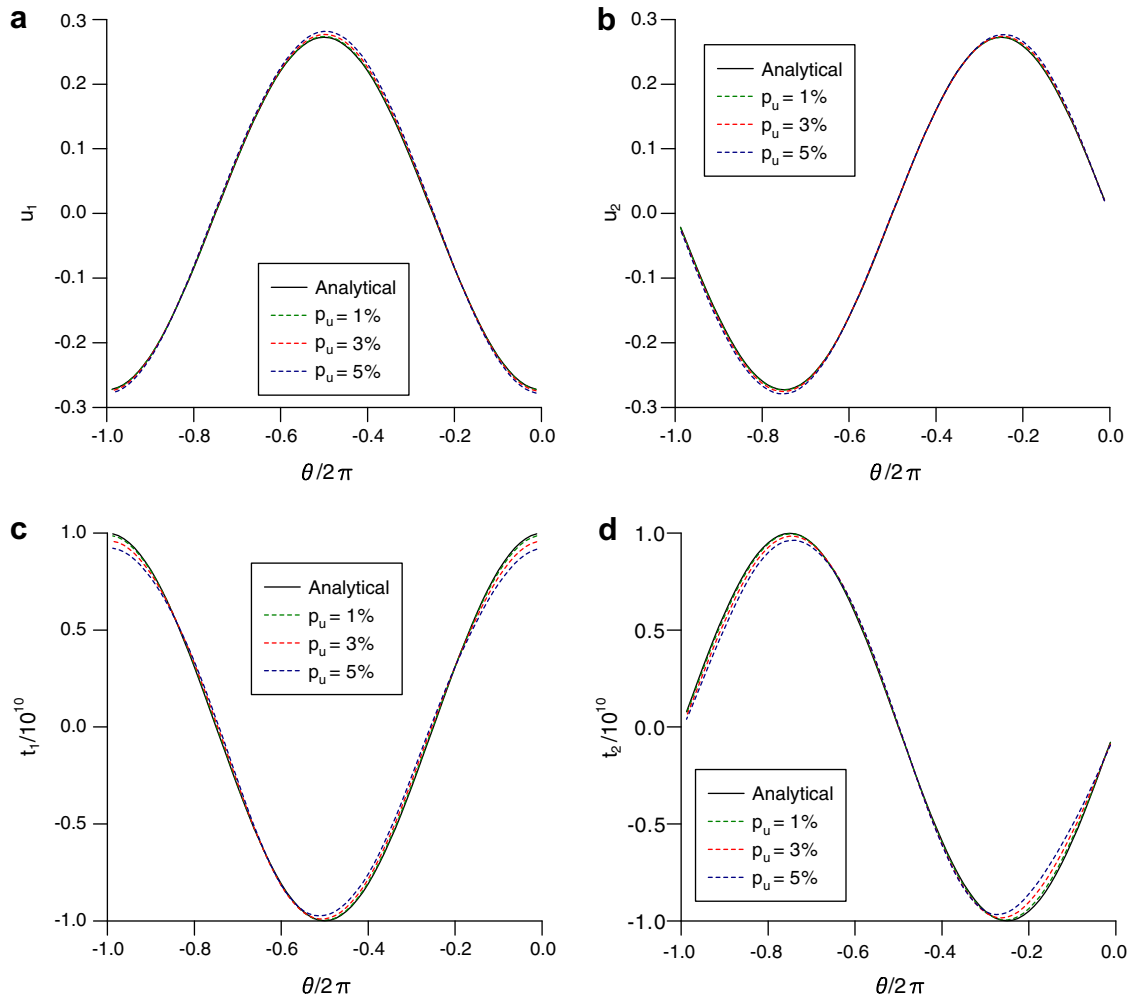

Fig. 5. The analytical and numerical displacements (a) u_1, and (b) u_2, and the analytical and numerical tractions (c) t_1, and (d) t_2, obtained on the under-specified boundary $\Gamma_1 \equiv \Gamma_{\text{out}}$, using the MEM, the stopping criterion given by Eq. (66) and various amounts of noise added into the displacement, $\mathbf{u}|_{\Gamma_0} \equiv \mathbf{u}|_{\Gamma_{\text{int}}}$, i.e. $p_{\mathbf{u}} \in \{1\%, 5\%, 10\%\}$, for Problem II.

on the inner boundary $\Gamma_1 \equiv \Gamma_{\text{int}}$ from Cauchy data on the outer boundary $\Gamma_0 \equiv \Gamma_{\text{out}}$. The numerical results obtained for the x_1- and x_2-components of the displacement vector on the under-specified boundary $\Gamma_1 \equiv \Gamma_{\text{int}}$ using the MEM, the regularizing stopping criterion (66) and various amounts of noise added into the displacement, $\mathbf{u}|_{\Gamma_0} \equiv \mathbf{u}|_{\Gamma_{\text{out}}}$, i.e. $p_{\mathbf{u}} \in \{1\%, 2\%, 3\%\}$, represent stable, convergent and very good approximations for their "exact" counterparts, as can be seen from Fig. 6(a) and (b), respectively. However, the numerical values retrieved for the x_1- and x_2-components of the traction vector on the under-specified boundary $\Gamma_1 \equiv \Gamma_{\text{int}}$ using the MEM are highly unstable, see Fig. 6(c) and (d), and this phenomenon has also been observed and reported by Háo and Lesnic (2000) and Marin et al. (2002b) when solving Cauchy problems for the two-dimensional Laplace equation and linear elasticity system, respectively, by employing the CGM.

From the numerical results presented in this section and illustrated in Figs. 4–6, it can be concluded that the stopping criterion developed in Section 5.4 has a regularizing effect and the numerical solution obtained by the combined MEM-BEM described in this paper is convergent and stable with respect to increasing the mesh size discretisation and decreasing the level of noise added into the input data, respectively. However, it should be mentioned that although the MEM-based numerical displacements obtained on the under-specified boundary Γ_1 are stable, convergent and very good approximations for their corresponding "exact" values, the numerically retrieved tractions on Γ_1 are unstable, provided that their associated "exact" values are discontinuous.
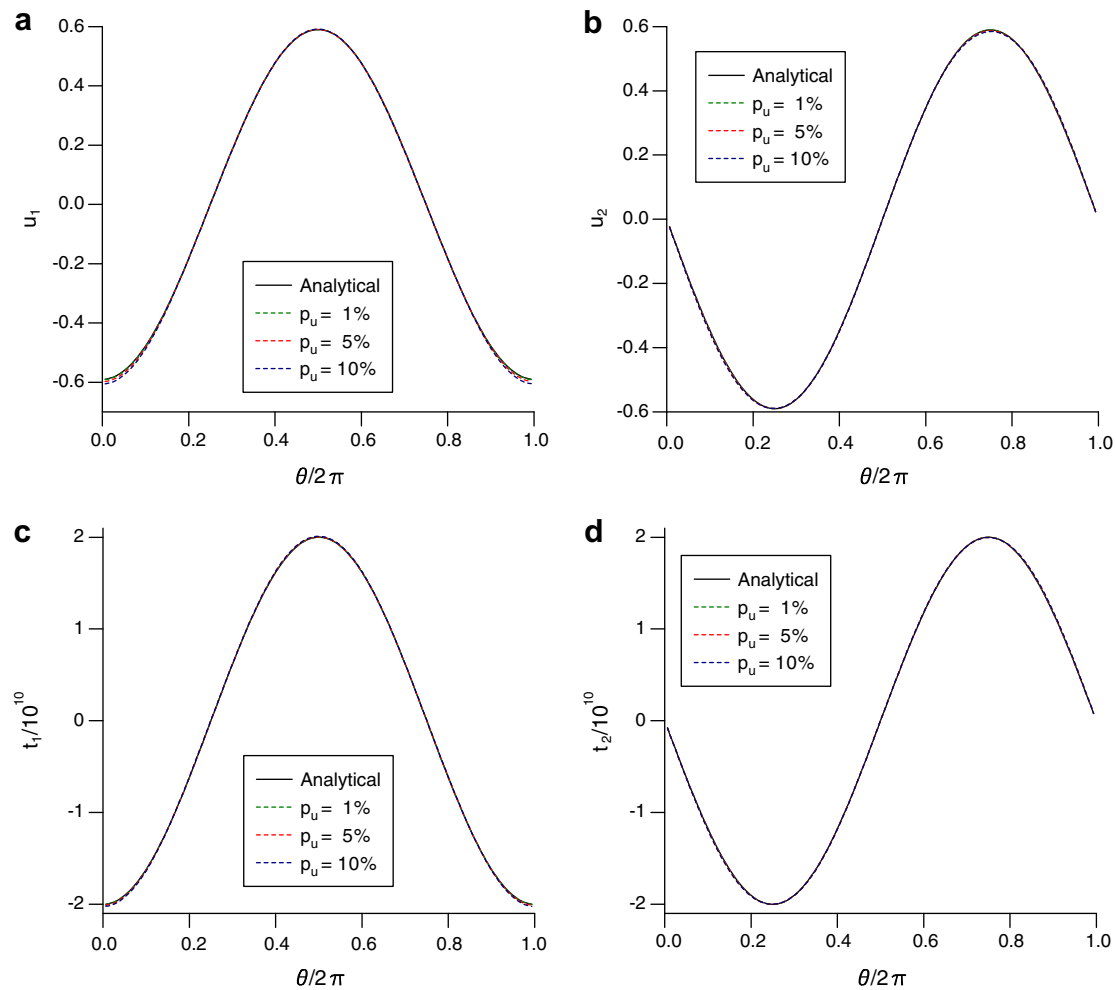

Fig. 6. The analytical and numerical displacements (a) u_1, and (b) u_2, and the analytical and numerical tractions (c) t_1, and (d) t_2, obtained on the under-specified boundary $\Gamma_1 \equiv \Gamma_{\text{int}}$ using the MEM, the stopping criterion given by Eq. (66) and various amounts of noise added into the displacement, $\mathbf{u}|_{\Gamma_0} \equiv \mathbf{u}|_{\Gamma_{\text{out}}}$, i.e. $p_{\mathbf{u}} \in \{1\%, 2\%, 3\%\}$, for Problem III.

5.6. Comparison with other iterative methods

It is the purpose of this section to compare the numerical results retrieved using the MEM, presented in Section 4.2, and its associated stopping rule given by Eq. (66), with those obtained using the other two iterative methods, namely the LFM and CGM, described in Sections 3.3 and 4.1, respectively, along with the stopping criterion described by Eq. (65). To do so, we set $N_{int} = N_{out}/2. = 80$ for both Problems I and II, and also consider a fixed level of noise added into the boundary displacement data, $\mathbf{u}|_{\Gamma_0}$, namely $p_{\mathbf{u}} = 5\%$ and $p_{\mathbf{u}} = 10\%$ in the case of Problems I and II, respectively. From the numerical experiments carried out in this study, the optimal value, τ_{opt}, for the parameter τ in the stopping rule (65) associated with the LFM and CGM was found to be $\tau_{opt} \approx 1.01$ for both these iterative methods.

Fig. 7(a)–(d) show the numerical solutions for the components of the displacement vector, u_1 and u_2, and traction vector, t_1 and t_2, respectively, in comparison with their corresponding analytical values, obtained using $p_{\mathbf{u}} = 5\%$, the MEM and its associated stopping rule Eq. (66), and the CGM and LFM, along with the stopping criterion described by Eq. (65), for Problem I. For this value of $p_{\mathbf{u}}$, the LFM, CGM and MEM are stopped after $k_{opt} = 332$, $k_{opt} = 4$ and $k_{opt} = 3$ iterations, respectively, as can be seen from Table 1 which presents the values of the optimal iteration number, k_{opt}, the corresponding accuracy errors, $e_{\mathbf{u}}^a(k_{opt})$ and $e_t^a(k_{opt})$, the convergence error, $e_{\mathbf{u}}^c(k_{opt})$, and the computational time, obtained using the CGM, LFM and MEM and various amounts of noise added into the boundary displacement data, i.e. $p_{\mathbf{u}} \in \{1\%, 2\%, 3\%, 4\%, 5\%\}$, for Problem I. From this table, as well as Fig. 7(a)–(d), it can be seen that in terms of accuracy, the CGM outperforms the LFM followed by the
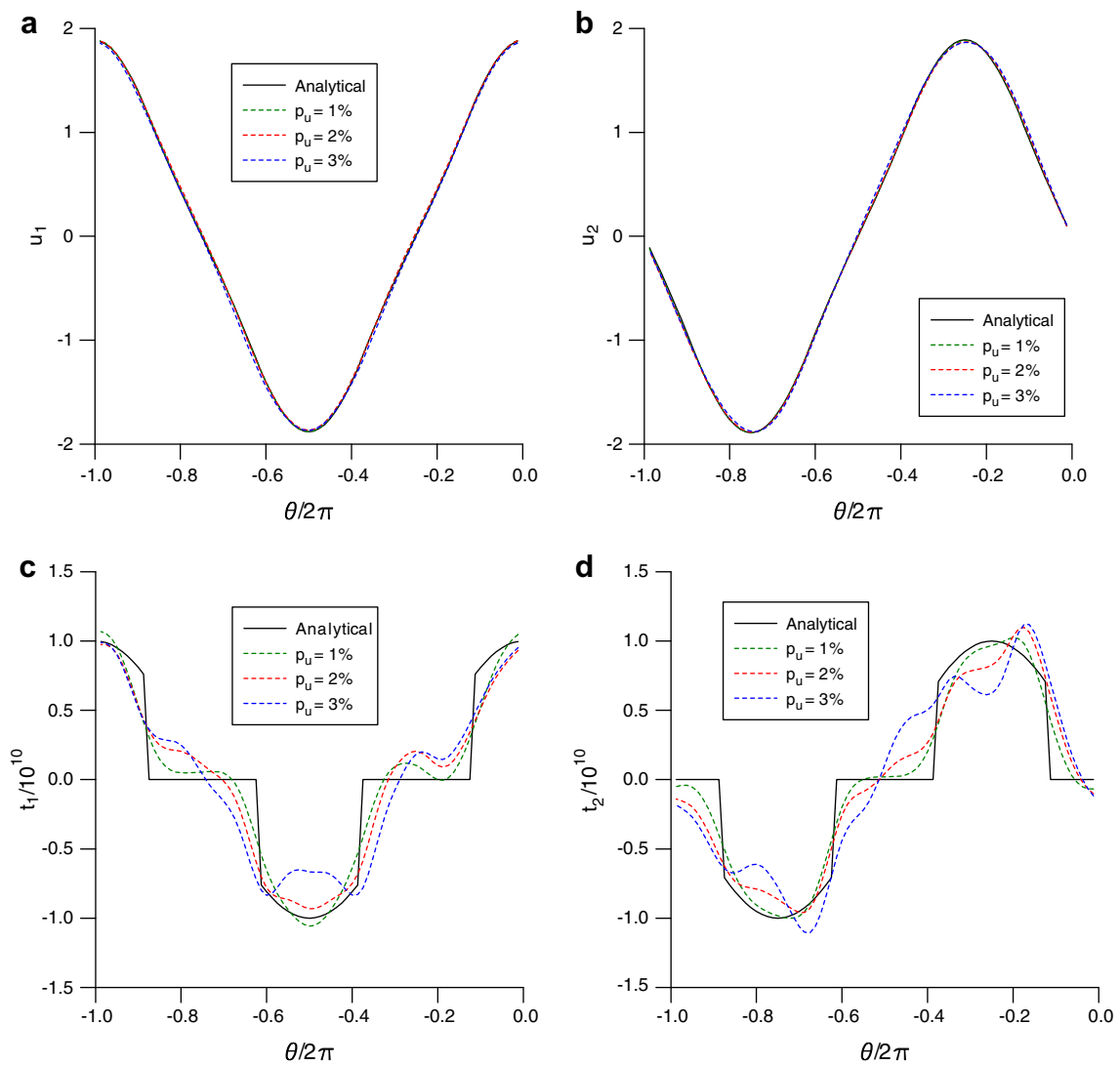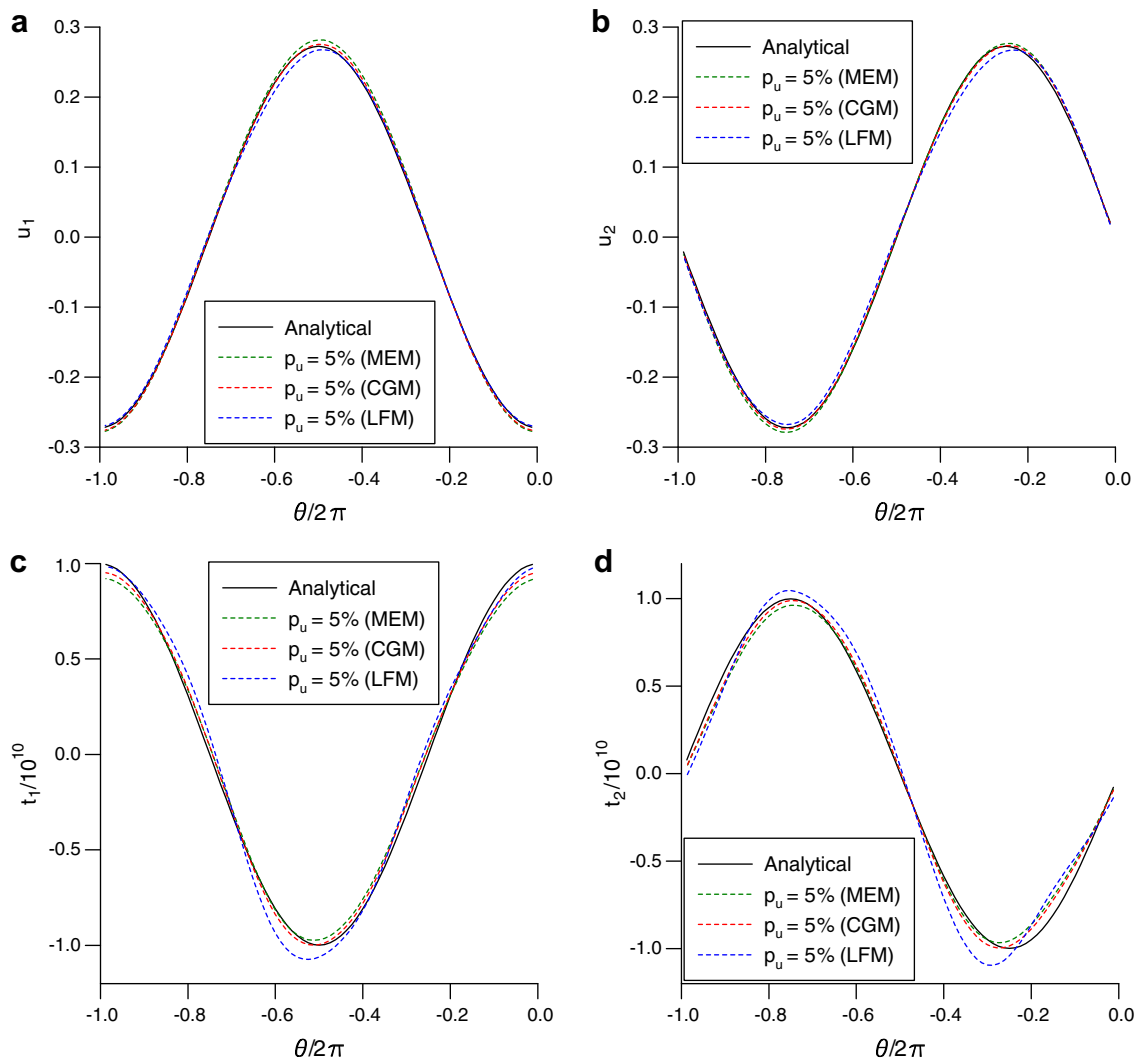

Fig. 7. The analytical and numerical displacements (a) u_1, and (b) u_2, and the analytical and numerical tractions (c) t_1, and (d) t_2, obtained on the underspecified boundary $\Gamma_1 \equiv \Gamma_{int}$ using $N_{out} = 160$ and $N_{int} = 80$ continuous linear boundary elements for discretising Γ_{out} and Γ_{int}, respectively, the CGM, LFM and MEM and $p_{\mathbf{u}} = 5\%$ noise added into the boundary displacement, $\mathbf{u}|_{\Gamma_0} \equiv \mathbf{u}\|_{\Gamma_{out}}$, for Problem I.

Table 1
The values of the optimal iteration number, k_{opt}, the corresponding accuracy errors, $e_u^a(k_{opt})$ and $e_t^a(k_{opt})$, the convergence error, $e_u^c(k_{opt})$, and the computational time, obtained using $N_{out} = 160$ and $N_{int} = 80$ continuous linear boundary elements for discretising the outer and inner boundaries, respectively, the CGM, LFM and MEM and various amounts of noise added into the boundary displacement data, i.e. $p_u \in \{1\%, 2\%, 3\%, 4\%, 5\%\}$, for Problem I.

| Method	p_u (%)	$e_u^a(k_{opt})$	$e_t^a(k_{opt})$	$e_u^c(k_{opt})$	k_{opt}	CPU time (s)
CGM	1	0.22489×10^{-2}	0.25491×10^{-1}	0.12281×10^{-1}	4	14.62
	2	0.44710×10^{-2}	0.50860×10^{-1}	0.24561×10^{-1}	4	15.44
	3	0.66979×10^{-2}	0.76257×10^{-1}	0.36841×10^{-1}	4	16.11
	4	0.89274×10^{-2}	0.10167×10^{0}	0.49120×10^{-1}	4	15.12
	5	0.11158×10^{-1}	0.12709×10^{0}	0.61399×10^{-1}	4	15.30
LFM	1	0.53911×10^{-2}	0.68589×10^{-1}	0.12457×10^{-1}	471	841.95
	2	0.10032×10^{-1}	0.12663×10^{0}	0.24908×10^{-1}	411	729.03
	3	0.14379×10^{-1}	0.17991×10^{0}	0.37381×10^{-1}	375	657.23
	4	0.18434×10^{-1}	0.22999×10^{0}	0.49822×10^{-1}	351	620.09
	5	0.22332×10^{-1}	0.27751×10^{0}	0.62276×10^{-1}	332	603.67
MEM	1	0.27749×10^{-2}	0.26377×10^{-1}	0.12573×10^{-1}	3	10.12
	2	0.60899×10^{-2}	0.55851×10^{-1}	0.25145×10^{-1}	3	10.27
	3	0.10001×10^{-1}	0.88937×10^{-1}	0.37718×10^{-1}	3	10.50
	4	0.14568×10^{-1}	0.12616×10^{0}	0.50290×10^{-1}	3	10.36
	5	0.19827×10^{-1}	0.16792×10^{0}	0.62862×10^{-1}	3	9.62
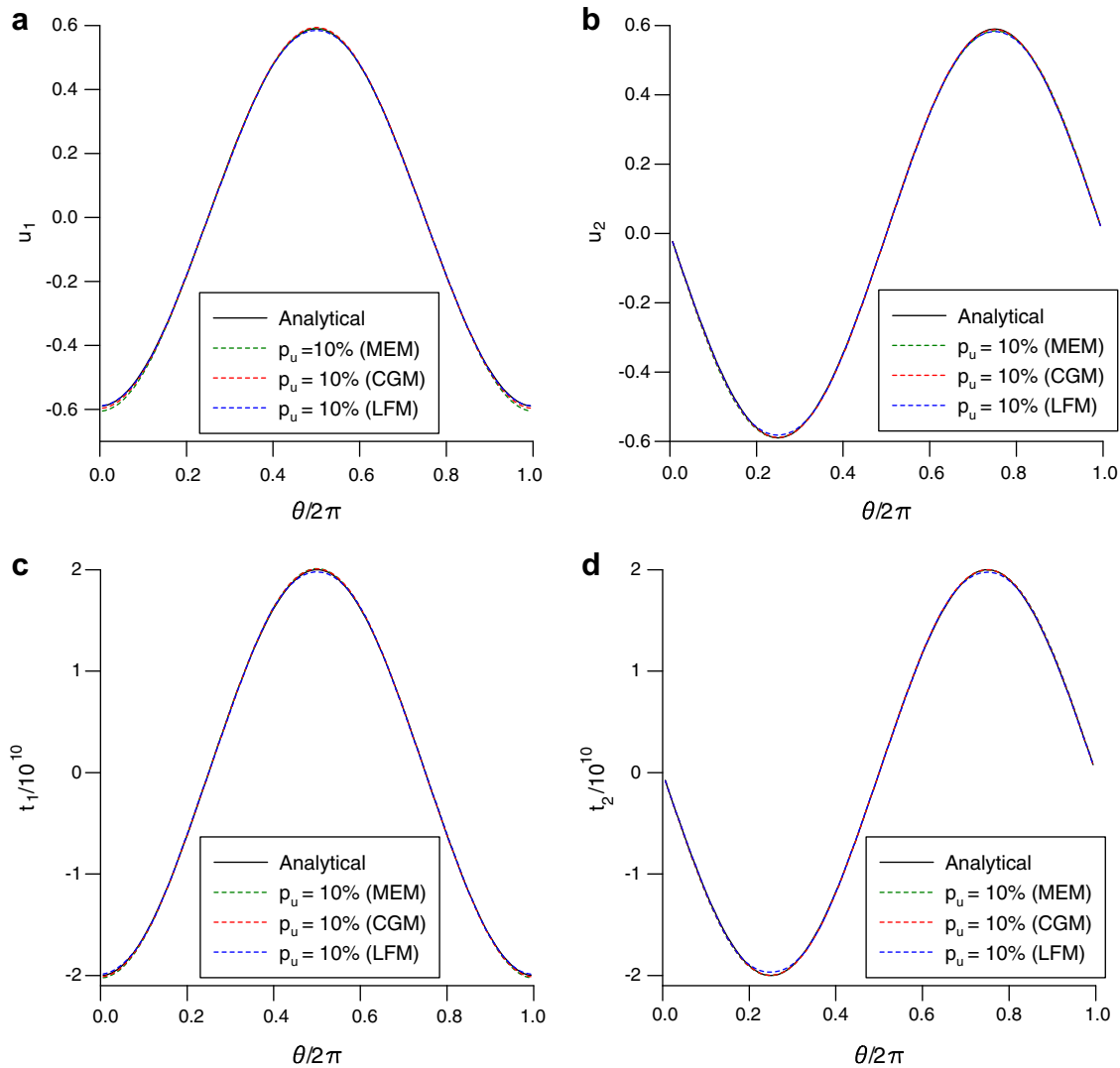
Fig. 8. The analytical and numerical displacements (a) u_1, and (b) u_2, and the analytical and numerical tractions (c) t_1, and (d) t_2, obtained on the under-specified boundary $\Gamma_1 \equiv \Gamma_{out}$, using $N_{out} = 160$ and $N_{int} = 80$ continuous linear boundary elements for discretising Γ_{out} and Γ_{int}, respectively, the CGM, LFM and MEM and $p_u = 10\%$ noise added into the boundary displacement, $\mathbf{u}|_{\Gamma_0} \equiv \mathbf{u}|_{\Gamma_{int}}$, for Problem II.

Table 2
The values of the optimal iteration number, k_{opt}, the corresponding accuracy errors, $e_{\mathbf{u}}^{a}(k_{opt})$ and $e_{\mathbf{t}}^{a}(k_{opt})$, the convergence error, $e_{\mathbf{u}}^{c}(k_{opt})$, and the computational time, obtained using $N_{out} = 160$ and $N_{int} = 80$ continuous linear boundary elements for discretising the outer and inner boundaries, respectively, the CGM, LFM and MEM and various amounts of noise added into the boundary displacement data, i.e. $p_{\mathbf{u}} \in \{1\%, 2\%, 3\%, 4\%, 5\%, 10\%\}$, for Problem II.

Method	$p_{\mathbf{u}}$ (%)	$e_{\mathbf{u}}^{a}(k_{opt})$	$e_{\mathbf{t}}^{a}(k_{opt})$	$e_{\mathbf{u}}^{c}(k_{opt})$	k_{opt}	CPU time (s)
CGM	1	0.18475×10^{-2}	0.49234×10^{-2}	0.26651×10^{-2}	3	11.62
	2	0.38609×10^{-2}	0.10446×10^{-1}	0.53288×10^{-2}	3	11.20
	3	0.58758×10^{-2}	0.15971×10^{-1}	0.79927×10^{-2}	3	11.89
	4	0.78906×10^{-2}	0.21495×10^{-1}	0.10657×10^{-1}	3	11.86
	5	0.99049×10^{-2}	0.27017×10^{-1}	0.13321×10^{-1}	3	11.97
	10	0.19170×10^{-1}	0.54604×10^{-1}	0.26641×10^{-1}	3	11.75
LFM	1	0.24561×10^{-2}	0.10152×10^{-1}	0.27574×10^{-2}	343	602.45
	2	0.45987×10^{-2}	0.18688×10^{-1}	0.55128×10^{-2}	310	562.20
	3	0.66081×10^{-2}	0.26572×10^{-1}	0.82633×10^{-2}	291	524.66
	4	0.85759×10^{-2}	0.34106×10^{-1}	0.11022×10^{-1}	277	507.05
	5	0.10509×10^{-1}	0.41375×10^{-1}	0.13786×10^{-1}	266	485.55
	10	0.19513×10^{-1}	0.74538×10^{-1}	0.27569×10^{-1}	233	428.27
MEM	1	0.37851×10^{-2}	0.76393×10^{-2}	0.30584×10^{-2}	2	7.83
	2	0.74459×10^{-2}	0.14671×10^{-1}	0.61145×10^{-2}	2	8.73
	3	0.11128×10^{-1}	0.21804×10^{-1}	0.91713×10^{-2}	2	8.58
	4	0.14830×10^{-1}	0.29030×10^{-1}	0.12229×10^{-1}	2	8.52
	5	0.18551×10^{-1}	0.36351×10^{-1}	0.15286×10^{-1}	2	7.88
	10	0.37452×10^{-1}	0.74380×10^{-1}	0.30582×10^{-1}	2	7.84

MEM for each level of noise considered. Moreover, all these iterative methods produce stable and reasonably accurate numerical solutions.

However, apart from the dependence on the parameter γ, and also as a consequence of the choice made for it (i.e. very small values for γ in order for the LFM to converge), the major disadvantage of the LFM is represented by the large number of iterations performed until the numerical solution on the under-specified boundary is obtained. Thus, especially for large-scale problems, this becomes an inconvenient with respect to the computational time required by this iterative method. For Problem I, the CPU times needed for the LFM, CGM and MEM to reach the numerical solutions for the displacement and traction vectors on Γ_1 were found to be 603.67, 15.30 and 9.62 s, respectively, with the mention that all numerical computations have been performed in FORTRAN 90 in double precision on a 3.00 GHz Intel Pentium 4 machine.

Similar results have been obtained using the three iterative methods compared in this section for Problem II and these are presented in Fig. 8(a)–(d) that show the analytical and numerical solutions for u_1, u_2, t_1 and t_2, respectively, with $p_{\mathbf{u}} = 10\%$. Also, the values of the optimal iteration number, k_{opt}, the corresponding accuracy errors, $e_{\mathbf{u}}^{a}(k_{opt})$ and $e_{\mathbf{t}}^{a}(k_{opt})$, the convergence error, $e_{\mathbf{u}}^{c}(k_{opt})$, and the computational time, obtained using the CGM, LFM and MEM and various amounts of noise added into the boundary displacement data, i.e. $p_{\mathbf{u}} \in \{1\%, 2\%, 3\%, 4\%, 5\%, 10\%\}$, for Problem II, are presented in Table 2. Overall, from Figs. 7 and 8, as well as Tables 1 and 2, we can conclude that stable and reasonably accurate numerical solutions are obtained by employing all iterative methods analysed in this study, with the mention that the CGM outperforms the MEM, whilst the latter outperforms the LFM, as far as the accuracy of the solutions and computational times are concerned.

6. Conclusions

In this paper, the Cauchy problem for the linear elasticity system with $L^2(\Gamma_0)^d$ boundary data was investigated numerically using yet another iterative method, namely the MEM. This rather weak requirements for the Cauchy data offers practical applicability of the proposed approach. An associated stopping criterion, necessary for ceasing the iterations at the point where the accumulation of noise becomes dominant and the errors in predicting the exact solution increase, was also developed. On using the BEM, the iterative parameter-free MEM, which reduced the Cauchy problem to solving a sequence of well-posed, mixed, boundary value problems in $L^2(\Omega)^d$, was numerically implemented for three benchmark inverse problems in a two-dimensional doubly connected domain occupied by a homogeneous isotropic linear elastic material. For such an elastic medium, the numerical results obtained using various numbers of boundary elements and various amounts of noise added into the input data showed that the MEM, in conjunction with the BEM, produces a convergent and stable numerical solution with respect to increasing the number of boundary elements and decreasing the amount of noise, respectively. It is important to mention that although the MEM-based numerical displacements obtained on the under-specified boundary Γ_1 are stable approximations for their corresponding "exact" values, the numerically retrieved tractions on Γ_1 are unstable, provided that the associated "exact" values for the latter are discontinuous on Γ_1.

Furthermore, the MEM was also compared with another two iterative methods, more precisely with a parameter-free procedure (CGM), as well as a parameter-dependent method (LFM), together with their associated regularizing stopping criteria, which were previously introduced by Marin et al. (2002b) and Marin and Lesnic (2005), respectively. It was shown that,

in terms of accuracy, the CGM outperforms the LFM, whilst the latter outperforms the MEM. The LFM requires the choice of the parameter γ in a suitable range in order to achieve the convergence of this numerical method. This is achieved by choosing a sufficiently small value for the parameter γ (in practice, $\gamma \approx 0.1$), which implies a much larger number of iterations until the numerical solution is obtained than those required by the parameter-free methods analysed in this paper. Consequently, especially for large-scale problems, the CGM and MEM are preferred to the LFM since the latter is quite slow in comparison with the aforementioned parameter-free methods as far as CPU times are concerned. To conclude, in terms of convergence rate, stability and accuracy, among the iterative methods analysed in this paper, the parameter-free methods MEM and CGM are recommended to be used, with a special mention for the latter. Future work will be related to the application of the MEM to solving numerically the Cauchy problem associated with other partial differential operators, such as the Helmholtz and modified Helmholtz operators.

References

Bastay, G., Kozlov, V.A., Turesson, B., 2001. Iterative methods for and inverse heat conduction problem. Journal of Inverse and Ill-Posed Problems 9, 375–388.

Brebbia, C.A., Telles, J.F.C., Wrobel, L.C., 1984. Boundary Element Techniques. Springer, London.

Comino, L., Marin, L., Gallego, R., 2007. An alternating iterative algorithm for the Cauchy problem in anisotropic elasticity. Engineering Analysis with Boundary Elements 31, 667–682.

Engl, H.W., Hanke, M., Neubauer, A., 1996. Regularization of Inverse Problems. Kluwer Academic Publications, Boston.

Hadamard, J., 1923. Lectures on Cauchy Problem in Linear Partial Differential Equations. Oxford University Press, London.

Hanke, M., 1995a. Conjugate Gradient Type Methods for Ill-Posed Problems. Longman Scientific and Technical, New York.

Hanke, M., 1995b. The minimal error conjugate gradient method is a regularization method. Proceedings of the American Mathematical Society 123, 3487–3497.

Háo, D.N., Reinhardt, H.-J., 1998. Gradient methods for inverse heat conduction problems. Inverse Problems in Engineering 6, 177–211.

Háo, D.N., Lesnic, D., 2000. The Cauchy problem for Laplace's equation via the conjugate gradient method. IMA Journal of Applied Mathematics 65, 199–217.

Huang, C.H., Shih, W.Y., 1997. A boundary element based solution of an inverse elasticity problem by conjugate gradient and regularization method. In: Proceedings of the 7th International Offshore Polar Engineering Conference, Honolulu, USA, pp. 338–395.

Johansson, T., 2000. Reconstruction of a Stationary Flow from Boundary Data. Dissertations No. 853, Linköping Studies in Science and Technology.

Johansson, T., Lesnic, D., 2007. An iterative method for the reconstruction of a stationary flow*. Numerical Methods for Partial Differential Equations 23, 998–1017.

Johansson, T., Lesnic, D., 2006a. A variational conjugate gradient method for determining the fluid velocity of a slow viscous flow. Applicable Analysis 85, 1327–1341.

Johansson, T., Lesnic, D., 2006b. Reconstruction of a stationary flow from incomplete boundary data using iterative methods. European Journal of Applied Mathematics 17, 651–663.

King, J.T., 1989. The minimal error conjugate gradient method for ill-posed problems. Journal of Optimization Theory and Applications 60, 297–304.

Knops, R.J., Payne, L.E., 1986. Theory of Elasticity. Pergamon Press, Oxford.

Koya, T., Yeih, W.C., Mura, T., 1993. An inverse problem in elasticity with partially overspecified boundary conditions. II. Numerical details. Transactions of the ASME. Journal of Applied Mechanics 60, 601–606.

Kubo, S., 1988. Inverse problems related to the mechanics and fracture of solids and structures. Japan Society of Mechanical Engineers (JSME) International Journal 31, 157–166.

Landau, L.D., Lifshits, E.M., 1986. Theory of Elasticity. Pergamon Press, Oxford.

Landweber, L., 1951. An iteration formula for Fredholm integral equations of the first kind. American Journal of Mathematics 73, 615–624.

Maniatty, A., Zabaras, N., Stelson, K., 1989. Finite element analysis of some elasticity problems. Journal of Engineering Mechanics Division ASCE 115, 1302–1316.

Marin, L., Elliott, L., Ingham, D.B., Lesnic, D., 2001. Boundary element method for the Cauchy problem in linear elasticity. Engineering Analysis with Boundary Elements 25, 783–793.

Marin, L., Elliott, L., Ingham, D.B., Lesnic, D., 2002a. Boundary element regularization methods for solving the Cauchy problem in linear elasticity. Inverse Problems in Engineering 10, 335–357.

Marin, L., Háo, D.N., Lesnic, D., 2002b. Conjugate gradient-boundary element method for the Cauchy problem in elasticity. Quarterly Journal of Mechanics and Applied Mathematics 55, 227–247.

Marin, L., Lesnic, D., 2002a. Regularized boundary element solution for an inverse boundary value problem in linear elasticity. Communications in Numerical Methods in Engineering 18, 817–825.

Marin, L., Lesnic, D., 2002b. Boundary element solution for the Cauchy problem in linear elasticity using singular value decomposition. Computer Methods in Applied Mechanics and Engineering 191, 3257–3270.

Marin, L., Elliott, L., Heggs, P.J., Ingham, D.B., Lesnic, D., Wen, X., 2003. Conjugate gradient-boundary element solution to the Cauchy problem for Helmholtz-type equations. Computational Mechanics 31, 367–377.

Marin, L., Lesnic, D., 2004. The method of fundamental solutions for the Cauchy problem in two-dimensional linear elasticity. International Journal of Solids and Structures 41, 3425–3438.

Marin, L., Elliott, L., Heggs, P.J., Ingham, D.B., Lesnic, D., Wen, X., 2004. BEM solution for the Cauchy problem associated with Helmholtz-type equations by the Landweber method. Engineering Analysis with Boundary Elements 28, 1025–1034.

Marin, L., 2005. A meshless method for solving the Cauchy problem in three-dimensional elastostatics. Computers & Mathematics with Applications 50, 73–92.

Marin, L., Lesnic, D., 2005. Boundary element-Landweber method for the Cauchy problem in linear elasticity. IMA Journal of Applied Mathemstics 18, 817–825.

Morozov, V.A., 1966. On the solution of functional equations by the method of regularization. Soviet Mathematics Doklady 167, 414–417.

Nemirovskii, A.S., 1986. Regularizing properties of the conjugate gradient method in ill-posed problems. USSR Computational Mathematics and Mathematical Physics 26, 7–16.

Schnur, D., Zabaras, N., 1990. Finite element solution of two-dimensional elastic problems using spatial smoothing. International Journal for Numerical Methods in Engineering 30, 57–75.

Yakhno, V.G., 1990. Inverse Problems for Differential Equations of Elasticity. Nauka Sibirsk. Otdel, Novosibirsk (in Russian).

Yeih, W.C., Koya, T., Mura, T., 1993. An inverse problem in elasticity with partially overspecified boundary conditions. I. Theoretical approach. Transactions of the ASME Journal of Applied Mechanics 60, 595–600.

Zabaras, N., Morellas, V., Schnur, D., 1989. Spatially regularized solution of inverse elasticity problems using the BEM. Communications in Applied Numerical Methods 5, 547–553.